The Potential and Flux Landscape Theory of Ecology

Article *in* The Journal of Chemical Physics · August 2012

DOI: 10.1063/1.4734305 · Source: PubMed

5 authors, including:

Li Xu
Chinese Academy of Sciences
11 PUBLICATIONS **688** CITATIONS
SEE PROFILE

Kun Zhang
Chinese Academy of Sciences
20 PUBLICATIONS **458** CITATIONS
SEE PROFILE

Jin Wang
Stony Brook University Hospital
87 PUBLICATIONS **2,052** CITATIONS
SEE PROFILE

The potential and flux landscape theory of evolution

Feng Zhang, Li Xu, Kun Zhang, Erkang Wang, and Jin Wang

Citation: J. Chem. Phys. **137**, 065102 (2012); doi: 10.1063/1.4734305
View online: http://dx.doi.org/10.1063/1.4734305
View Table of Contents: http://jcp.aip.org/resource/1/JCPSA6/v137/i6
Published by the American Institute of Physics.

The potential and flux landscape theory of evolution

Feng Zhang,[1,2,a)] Li Xu,[1,a)] Kun Zhang,[1] Erkang Wang,[1,b)] and Jin Wang[1,2,3,c)]
[1]*State Key Laboratory of Electroanalytical Chemistry, Changchun Institute of Applied Chemistry, Chinese Academy of Sciences, Changchun, Jilin 130022, People's Republic of China*
[2]*College of Physics, Jilin University, Changchun, Jilin 130012, People's Republic of China*
[3]*Department of Chemistry, Physics and Applied Mathematics, State University of New York at Stony Brook, Stony Brook, New York 11794-3400, USA*

(Received 16 April 2012; accepted 24 June 2012; published online 8 August 2012)

We established the potential and flux landscape theory for evolution. We found explicitly the conventional Wright's gradient adaptive landscape based on the mean fitness is inadequate to describe the general evolutionary dynamics. We show the intrinsic potential as being Lyapunov function(monotonically decreasing in time) does exist and can define the adaptive landscape for general evolution dynamics for studying global stability. The driving force determining the dynamics can be decomposed into gradient of potential landscape and curl probability flux. Non-zero flux causes detailed balance breaking and measures how far the evolution from equilibrium state. The gradient of intrinsic potential and curl flux are perpendicular to each other in zero fluctuation limit resembling electric and magnetic forces on electrons. We quantified intrinsic energy, entropy and free energy of evolution and constructed non-equilibrium thermodynamics. The intrinsic non-equilibrium free energy is a Lyapunov function. Both intrinsic potential and free energy can be used to quantify the global stability and robustness of evolution. We investigated an example of three allele evolutionary dynamics with frequency dependent selection (detailed balance broken). We uncovered the underlying single, triple, and limit cycle attractor landscapes. We found quantitative criterions for stability through landscape topography. We also quantified evolution pathways and found paths do not follow potential gradient and are irreversible due to non-zero flux. We generalized the original Fisher's fundamental theorem to the general (i.e., frequency dependent selection) regime of evolution by linking the adaptive rate with not only genetic variance related to the potential but also the flux. We show there is an optimum potential where curl flux resulting from biotic interactions of individuals within a species or between species can sustain an endless evolution even if the physical environment is unchanged. We offer a theoretical basis for explaining the corresponding Red Queen hypothesis proposed by Van Valen. Our work provides a theoretical foundation for evolutionary dynamics.
 [http://dx.doi.org/10.1063/1.4734305]

I. INTRODUCTION

The fundamental nature of biology is determined by evolution. Understanding the evolution is one of the greatest challenges in modern science. Tremendous efforts have been made on uncovering the laws of evolution. Darwin first formulated the theory of evolution by means of natural selection to explain the adaptation and speciation.[1] Fisher proposed the fundamental theorem of natural selection to indicate the increase rate of mean fitness by natural selection is equal to its genetic variance in fitness.[2] Wright proposed the fitness landscape concept in which the evolutionary adaptation may be seen as a hill-climbing process on the mean fitness landscape until a local mean fitness peak is reached.[3] Wright's fitness landscape and Fisher's fundamental theorem of natural selection have been widely used to interpret the adaptation as the mean fitness maximization.

However, the evolutionary dynamics is complex. Wright's fitness landscape as the gradient evolutionary dynamics[3] only applies to extremely simple cases in which all the interactions among individuals are neglected. The ubiquitous biotic interactions of individuals within a species or between species can give rise to the frequency-dependent selection. In this case, evolution dynamics no longer follows the gradient of the mean fitness. The coevolving systems may enter into an endless cycle rather than reaching the mean fitness peaks. This was proposed by Van Valen as Red Queen hypothesis[4] (details in Appendixes): the biotic interactions between different species provide a driving force resulting in endless evolution for some species even if the physical environment is unchanged. The Red Queen hypothesis cannot be explained by the conventional evolutionary theory. The Red Queen effect is appreciated for rationalizing why sexual reproduction occurs[5–7] and supported by some empirical evidences.[8–10] Despite this, the underlying mechanism of Red Queen effect is still unclear and remains as a rather open problem.[7,11]

It is a great challenge to find the true adaptive landscape reaching the optima and address the issues on global stability and robustness of the evolutionary dynamics.[12–23] In equilibrium systems, the global nature of the systems

a)Feng Zhang and Li Xu contributed equally to this work.
b)Electronic mail: ekwang@ciac.jl.cn.
c)Electronic mail: jin.wang.1@stonybrook.edu.

is characterized by the potential landscape which is often known or given *a priori* (such as interactions among atoms in proteins and extremely simple evolution models). The potential landscape is linked with the equilibrium probability distribution by Boltzmann relationships. With the potential, one can obtain free energy and explore the global thermodynamic stability of the system. Furthermore, the local dynamics is determined by the potential gradient reflecting the local slope of the landscape. The thermodynamic stability and the dynamics together give a global description.

The evolutionary dynamics, however, is often non-equilibrium in nature and in general does not have a gradient potential as in the equilibrium case. So it is hard to explore the global characteristic without the potential landscape. Many people argue against the existence of adaptive landscape[24] due to the possible existence of limit cycle (an example is illustrated through the Red Queen effect[4]) in evolution since the fitness searches for optimum and therefore cannot go back to itself. Even with the potential landscape, the link to the global characterization through probability distribution and furthermore the dynamics is unclear. In practice, evolution is often of this type.[24–26] Then the question is how we can study the global properties of these non-equilibrium evolutionary dynamics in a physical way.

One hint comes from the fact that the evolutionary dynamics is not in isolation. There are always intrinsic and extrinsic fluctuations around.[24–26] So, its probability distribution becomes essential. The steady state probability distribution can give a global characterization of the evolution.[12–22,24–26] The question is then how is that linked with the potential and dynamics of the evolution.

We developed a potential-flux landscape theory for evolution to explore the global dynamics. We found the driving force can be decomposed into two terms: one comes from the gradient of the non-equilibrium potential directly related to steady state probability distribution and the other comes from the curl probability flux leading to the breakdown of the detailed balance. While the potential landscape describes global natures of the system, the local dynamics is determined by both the gradient of non-equilibrium potential and the curl probability flux.[21] This is very different from the gradient alone nature of Wright's fitness landscape in determining the evolutionary dynamics. In fact, under the extreme condition of the frequency independent selection, the non-equilibrium potential reduces to Wright's fitness landscape without flux.

While non-equilibrium potential can be identified, one important question is whether or not the non-equilibrium potential is a Lyapunov function (monotonically changing in time, so that the corresponding potential function can be well defined and the evolutionary dynamics always search for the minima of the potential to settle) which is required to characterize the global behavior and address the global stability as in the equilibrium case. We construct the non-equilibrium potential landscape at finite fluctuations (called population potential, U). We take the zero fluctuation limit to obtain the intrinsic potential landscape (called intrinsic potential ϕ_0) and directly identify that as the Lyapunov function.[12–22,27] As a Lyapunov function, the intrinsic potential landscape can be defined as the general adaptive landscape for evolution. Furthermore, we explored the quantitative relationships between the driving force from gradient of the intrinsic potential and the one from the probability flux, and found they are orthogonal to each other resembling the electric and magnetic forces on the electrons.

We developed non-equilibrium thermodynamics to characterize the global properties of the evolution system.[17,27–30] Based on that we construct the underlying energy, entropy, and free energy. We can see the system entropy may not always increase. We found the intrinsic non-equilibrium free energy defined here always monotonically decreases in time for the evolutionary dynamics.[17,27–30] By exploring the non-equilibrium free energy in time and steady state, we analyzed the global stability of the evolution and associated phases as well as the phase transitions in between.

We explored an example of three allele evolution system with frequency dependent selection, to characterize quantitatively the global nature of evolution by uncovering the underlying non-equilibrium potential, the flux, and non-equilibrium free energy. We found four different phases in different parameter regimes: monostable phase, limit cycle phase, limit cycle and tristable phase, and tristable phase. We found the quantitative criterion for stability. We further investigated the quantitative relationship between the topography of the underlying landscape and the escape time from the basin. Since the escape time is a measure of the communication between the current state to the other states of the system (for example, from one attractor to another), the landscape topography can give a quantitative measure of the global stability. The slope against the roughness of the landscape determines the stability of the single attractor. The barrier heights between the basins of attractions or limit cycle attractors are correlated with escape time from the basins of attractions, which determines the stability of multiple attractors. While the gradient force attracts the evolution down to the limit cycle attractor, the curl flux is the driving force for the actual coherent oscillation along the limit cycle. Our potential and flux landscape provides a natural solution and explanation to the limit cycle in evolution. In contrast, Wright's adaptive fitness landscape theory cannot explain the presence of the limit cycle in evolution.

We explored how the landscape changes with respect to the system parameters. We also explored how the non-equilibrium free energy links with the different phases and phase transitions of the evolution with respect to parameters changes. These explained how the stability and robustness of evolution change under different conditions.

Quantifying the pathways for evolution is critical in understanding the evolution history and underlying origin, but yet not well explored. We quantified the evolutionary pathways through path integrals. We found that evolutionary paths do not follow potential gradient and therefore do not necessarily pass through the saddle point or transition state caused by curl flux. Furthermore, the evolution paths are irreversible due to again the non-zero flux.

We further generalized the Fisher's fundamental theorem of natural selection[2] to the general (including frequency dependent selection) regime of evolution linking the adaptive rate with not only the additive genetic variance related to the

intrinsic potential but also the flux. We discussed the Red Queen hypothesis[4] in our potential-flux landscape theory. We attribute the non-zero flux resulting from biotic interactions as the origin for the Red Queen effect of sustaining the endless evolution even when the potential function already reaches the optima.

II. THE POTENTIAL-FLUX LANDSCAPE THEORY AND NON-EQUILIBRIUM THERMODYNAMICS FOR GENERAL DYNAMICAL SYSTEMS

We will establish a potential and flux landscape theory and non-equilibrium thermodynamics for the general dynamical systems to address the issues of global stability, function, and robustness and set the theoretical basis for explaining the origin of limit cycle and Red Queen effect in evolution.

A. Driving force decomposition into gradient of potential landscape and flux for general dynamical systems

The deterministic dynamics of the general dynamical systems can be described by a set of nonlinear ordinary differential equations. But, a real system is often in fluctuations due to intrinsic and extrinsic noises. The stochastic dynamics is usually studied via stochastic differential equation:[31] $d\mathbf{x} = \mathbf{F}(\mathbf{x})dt + \mathbf{g} \cdot d\mathbf{W}$, where $\mathbf{x} = \{x_i | 1 \leq i \leq n\}$ is the state vector of a system with n degrees of freedoms (in evolution this variable is often refereed to as population or species density), $\mathbf{F}(\mathbf{x})$ is the deterministic driving force, $\mathbf{W}$ describes an independent Wiener process which is coupled through the matrix $\mathbf{g}$. To obtain the statistical property, we can track the long time evolution via solving the stochastic differential equation. Alternatively, we can obtain the probability distribution $P(\mathbf{x}, t)$ via solving the Fokker-Planck equation:

$$\partial P/\partial t = -\nabla \cdot \mathbf{J} = -\nabla \cdot [\mathbf{F}P - (1/2)\nabla \cdot ((\mathbf{g} \cdot \mathbf{g}^{\mathbf{T}})P)]. \quad (1)$$

We take $(1/2)(\mathbf{g} \cdot \mathbf{g}^{\mathbf{T}}) = D\mathbf{D}$, where D is a scale constant giving the magnitude of the fluctuations and $\mathbf{D}$ represents the scaled diffusion matrix giving a quantitative measure of the fluctuations.

The steady state probability distribution $P_{ss} = P(t \to \infty)$ can be solved from $\partial P/\partial t = -\nabla \cdot \mathbf{J} = 0$. We define a steady state probability flux $\mathbf{J_{ss}} = \mathbf{F}P_{ss} - D\nabla \cdot (\mathbf{D}P_{ss}) = P_{ss}(\mathbf{F} - D\nabla \cdot \mathbf{D} + D\mathbf{D} \cdot \nabla U)$, where the population potential $U = -\ln P_{ss}$ which is analogous to the Boltzmann law. The steady state probability flux is divergent free due to the steady state conditions. Divergent free flux has no sinks or leaks and so does not have a place to start or end. Thus the flux has no choice but posses a curl nature, rotating around. The deterministic driving force can be decomposed into three terms: $\mathbf{F} = -D\mathbf{D} \cdot \nabla U + \mathbf{J}_{ss}/P_{ss} + D\nabla \cdot \mathbf{D}$. The first term is the gradient of the potential U, the second term is from the steady state probability flux and the third term comes from the divergence of the diffusion matrix which represents the damping force from the fluctuations and can be absorbed with the total driving force.

When $\mathbf{J}_{ss} = 0$, the detailed balance is preserved and the equilibrium state is reached. The global stability is therefore determined by the equilibrium probability landscape, and the dynamics is determined by the force from the gradient of the potential and the divergence of diffusion matrix. On the other hand, when $\mathbf{J}_{ss} \neq 0$, the detailed balance is broken and the system becomes non-equilibrium. In this situation, the global stability can be addressed through the population potential landscape $U = -\ln P_{ss}$ while the local dynamics is determined by the gradient U, along with the divergence of diffusion matrix, and the non-zero flux of the system breaking the detailed balance.

Then, how to judge a system is in equilibrium or non-equilibrium from them? The system is in equilibrium, if $\mathbf{J}_{ss} = P_{ss}(\mathbf{F} - D\nabla \cdot \mathbf{D} + D\mathbf{D} \cdot \nabla U) = 0$. This implies

$$\nabla \times [\mathbf{D}^{-1} \cdot (\mathbf{F} - D\nabla \cdot \mathbf{D})] = 0. \quad (2)$$

On the contrary, if $\nabla \times [\mathbf{D}^{-1} \cdot (\mathbf{F} - D\nabla \cdot \mathbf{D})] \neq 0$, the non-zero steady state probability flux, $\mathbf{J}_{ss} \neq 0$, breaks the detailed balance.

B. The Lyapunov function and intrinsic potential landscapes for general dynamical systems

The challenge of dynamical systems is how we will characterize it globally in a physical way. Can we find the potential landscape with the property of Lyapunov function and use it to study the global function, stability, and robustness of evolution?[12–22,27] We will discuss in detail here on the existence and construction of the such a potential landscape as Lyapunov function.

In order to see the underlying intrinsic potential, we can reduce the effect of the fluctuation by taking $D \ll 1$. In this case, we can expand the population potential $U(\mathbf{x})$ with respect to the fluctuation strength D as the form:[13,14,30,32] $U(\mathbf{x}) = [\sum_{k=0}^{\infty} D^k \phi_k(\mathbf{x})]/D = \phi_0(\mathbf{x})/D + \phi_1(\mathbf{x}) + D\phi_2(\mathbf{x}) + \cdots$. Consequently, $P_{ss}(\mathbf{x}) = (1/Z)\exp[-(\sum_{k=0}^{\infty} D^k \phi_k(\mathbf{x}))/D]$ and $Z = \int \exp[-(\sum_{k=0}^{\infty} D^k \phi_k(\mathbf{x}))/D]d\mathbf{x}$. Doing this has four fold purposes. First is with the fluctuation strengths approaching to zero limit, we should recover the deterministic dynamic equations. The question is whether we can construct a potential landscape for the general non-equilibrium dynamics. If so, this will give an intrinsic potential which has Lyapunov property for the corresponding deterministic dynamics and depends on the nature of the driving force of the systems without explicit dependence on fluctuation strengths. Second, for real system, the fluctuations are often finite and none-zero. But for a large set of the systems the fluctuations often relatively weak. Then the weak fluctuation approximation through expansions upon fluctuation strengths D is able to deal with the situations. Third, with the D expansions, one can control the strength of the fluctuation and see how the probability distribution changes with fluctuations. Forth, when the fluctuations are large, one can directly solve the full probabilistic equation without weak fluctuation approximation.

By inserting the expanded expression of P into the steady state Fokker-Plank equation and compare the coefficients with the same power D on both sides of the equation, we obtain a set of equations about $\phi_i(\mathbf{x})$.[32] The equation for leading order expansion D^{-1} is as follows:

$$\mathbf{F} \cdot \nabla \phi_0 + \nabla \phi_0 \cdot \mathbf{D} \cdot \nabla \phi_0 = 0. \quad (3)$$

The solution ϕ_0 does not depend on fluctuation strength D. We can see the ϕ_0 monotonously decrease along a deterministic path due to the positive definite diffusion matrix $\mathbf{D}$:

$$d\phi_0(\mathbf{x})/dt = \mathbf{F}\cdot\nabla\phi_0 = -\nabla\phi_0\cdot\mathbf{D}\cdot\nabla\phi_0 \le 0. \quad (4)$$

The evolutionary process will not stop until the system reaches the attractor states that satisfied the $\nabla\phi_0 = 0$. For point attractors, ϕ_0 settles at minimum values. For continuous attractors such as line attractors, limit cycles or strange attractors, the values of ϕ_0 must settle at constant values. This is because, if the ϕ_0 values on continuous attractors are different, then it implies the right side of the above equation is not zero in between these values and ϕ_0 has not settled ($d\phi_0/dt \neq 0$) which is obviously not true. So, $d\phi_0/dt = 0$ requires the ϕ_0 are at constant values on continuous attractors. Due to the monotonic decreasing nature, ϕ_0 is a Lyapunov function. Finding the Lyapunov function is crucial for studying the global stability for the dynamical systems.

What is the physical meaning of ϕ_0? First, ϕ_0 itself with a dimension of D now can be linked with the steady state probability $P_{ss} \sim \exp(-\phi_0/D)$ at small noise limit. So, ϕ_0 links to the probability which characterizes the steady state globally. Second, ϕ_0 itself is a Lyapunov function monotonically decreasing which can be used to study the global stability. With both of these above mentioned properties, ϕ_0 now has the physical meaning of the non-equilibrium potential characterizing the global stability for the general dynamical systems, such as the evolutionary systems. So, we call the ϕ_0 non-equilibrium intrinsic potential.

C. Force decomposition and relationship between intrinsic probability flux and intrinsic potential

In the zero-fluctuation limit, $D \to 0$, we can also expand the steady state probability flux $\mathbf{J}_{ss}$ in terms of the fluctuation strengths D to obtain its leading order: $(\mathbf{J}_{ss}/P_{ss})|_{D\to 0} = \mathbf{F} + \mathbf{D}\cdot\nabla\phi_0$. We define the intrinsic flux velocity, $\mathbf{V} = (\mathbf{J}_{ss}/P_{ss})|_{D\to 0}$. From Eq. (3), we can see

$$\mathbf{V}\cdot\nabla\phi_0 = 0. \quad (5)$$

This implies that the gradient of the non-equilibrium intrinsic potential ϕ_0 is perpendicular to the intrinsic flux (or intrinsic flux velocity) in the zero-fluctuation limit. We can also look for the divergence of the intrinsic flux velocity which satisfies

$$\nabla\cdot\mathbf{V} = 0. \quad (6)$$

That is the intrinsic flux velocity is divergent free.

In the zero-fluctuation or deterministic dynamics limit, the driving force can be decomposed into both gradient of intrinsic potential ϕ_0 and the intrinsic flux velocity $\mathbf{V}$:

$$\mathbf{F} = -\mathbf{D}\cdot\nabla\phi_0 + \mathbf{V}. \quad (7)$$

D. Non-equilibrium thermodynamics, intrinsic energy, entropy, and free energy of general dynamical systems

For equilibrium systems, once the potential energy is known, we can find the equilibrium probability distribution and construct the partition function as well as the corresponding entropy and free energy. For non-equilibrium systems, the potential function is not known *a priori*. The question is can we construct the thermodynamics for the non-equilibrium dynamical system? As we have already seen, the non-equilibrium intrinsic potential is related to the steady state probability distribution at the zero-fluctuation limit, $\mathcal{P}_{ss}(\mathbf{x}) = P_{ss}(\mathbf{x})|_{D\to 0} = \exp(-\phi_0/\mathcal{D})/\mathcal{Z}$, where $\mathcal{D} = D|_{D\to 0}$ and $\mathcal{Z}$ is the intrinsic partition function defined as $\mathcal{Z} = \int \exp(-\phi_0/\mathcal{D})d\mathbf{x}$. From it, we can get $\phi_0 = -\mathcal{D}\ln(\mathcal{Z}\mathcal{P}_{ss})$. Notice that the intrinsic partition function $\mathcal{Z}$ is not dependent on time t. In analogy with the equilibrium system, we can define and quantify the intrinsic entropy of the deterministic non-equilibrium dynamical system as:[16–18,27–29] $\mathcal{S} = -\int \mathcal{P}(\mathbf{x},t)\ln\mathcal{P}(\mathbf{x},t)d\mathbf{x}$, where $\mathcal{P}(\mathbf{x},t) = P(\mathbf{x},t)|_{D\to 0}$. Further more, we can also define the intrinsic energy $\mathcal{E}$ of the non-equilibrium dynamical system as: $\mathcal{E} = \int \phi_0\mathcal{P}(\mathbf{x},t)d\mathbf{x} = -\mathcal{D}\int \ln(\mathcal{Z}\mathcal{P}_{ss})\mathcal{P}(\mathbf{x},t)d\mathbf{x}$. A natural definition of the intrinsic free energy $\mathcal{F}$ of the non-equilibrium system would be: $\mathcal{F} = \mathcal{E} - \mathcal{D}\mathcal{S} = \mathcal{D}[\int \mathcal{P}(\mathbf{x},t)\ln(\mathcal{P}(\mathbf{x},t)/\mathcal{P}_{ss})\,d\mathbf{x} - \ln\mathcal{Z}]$. If we consider the time evolution of the entropy and ask the question whether or not for the non-equilibrium system, the entropy of the non-equilibrium system is maximized, we can explore the derivatives of the entropy.[16–18,27–30]

The change of the entropy in time can be divided into two terms: $\dot{S} = \dot{S}_t - \dot{S}_e$ where entropy production rate, $\dot{S}_t = \int d\mathbf{x}(\mathbf{J}\cdot(D\mathbf{D})^{-1}\cdot\mathbf{J})/P$, is positive or zero, and heat dissipation rate or entropy flow rate to the non-equilibrium system from the environments can be either positive or negative: $\dot{S}_e = \int d\mathbf{x}(\mathbf{J}\cdot(D\mathbf{D})^{-1}\cdot\mathbf{F}')$, where the effective force $\mathbf{F}' = \mathbf{F} - D\nabla\cdot\mathbf{D}$. If we interpret $\dot{S}$ as the entropy change of the non-equilibrium system, then, the $\dot{S}_t$ has the physical meaning of the total entropy change of the system and environments which is always non-negative consistent with the thermodynamic second law. On the other hand, we can see the non-equilibrium system entropy can be increased or decreased due to the entropy flow from or to the environments. This gives the chance to create order. So the system entropy of the non-equilibrium is neither always increasing nor always maximized.

On the other hand, we can explore the derivative of intrinsic free energy with respect to time (details in Appendixes):[16–18,27–30]

$$\frac{d\mathcal{F}}{dt} = -\mathcal{D}^2\int \nabla\ln\left(\frac{\mathcal{P}}{\mathcal{P}_{ss}}\right)\cdot\mathbf{D}\cdot\nabla\ln\left(\frac{\mathcal{P}}{\mathcal{P}_{ss}}\right)\mathcal{P}d\mathbf{x} \le 0. \quad (8)$$

The intrinsic free energy of the non-equilibrium system $\mathcal{F}$ always decreases in time until reaching the minimum value $\mathcal{F} = -\mathcal{D}\ln\mathcal{Z}$. This can be understood as the second law of thermodynamics for non-equilibrium systems. Therefore, the intrinsic free energy is a Lyapunov function suitable to explore the global stability of the non-equilibrium system. Although the system entropy is not necessarily maximized, the intrinsic free energy does minimize itself. This may provide a design principle for the complex dynamical systems searching for optimum.

Having addressed such intrinsic free energy, we can explore the non-equilibrium nature of the steady state such as global stability. This can be done through the investigation of how the intrinsic energy, entropy, and free energy of the

non-equilibrium systems change with respect to fluctuation strengths D and the underlying system parameters. The intrinsic system entropy $\mathcal{S}_{ss} = -\int \mathcal{P}_{ss}(\mathbf{x})\ln\mathcal{P}_{ss}(\mathbf{x})d\mathbf{x}$ and intrinsic energy $\mathcal{E}_{ss} = \int \phi_0\mathcal{P}_{ss}(\mathbf{x})d\mathbf{x} = -\mathcal{D}\int \ln(\mathcal{Z}\mathcal{P}_{ss})\mathcal{P}_{ss}(\mathbf{x})d\mathbf{x}$ as well as the intrinsic free energy $\mathcal{F}_{ss} = -\mathcal{D}\ln\mathcal{Z}$ at steady state can be naturally defined with the probability in time replaced as steady state probability as shown above.[16,19] So, the intrinsic free energy of the non-equilibrium system at steady state would be $\mathcal{F}_{ss} = -\mathcal{D}\ln\mathcal{Z} = \mathcal{E}_{ss} - \mathcal{D}\mathcal{S}_{ss}$. We can see this as first law of thermodynamics for non-equilibrium systems. We notice that here the fluctuation strength D plays the role of temperature for the non-equilibrium systems in analogy to the equilibrium case. We can explore the non-equilibrium thermodynamic behavior when changing D. We expect at high fluctuations, entropy and disorder dominates and at low fluctuations, energy and order dominates. Therefore, non-equilibrium phase transitions may occur from disorder to order as fluctuation decreases (vice versa). The non-equilibrium phase transition may also occur when the system parameters change which can significantly influence the energy and entropy balance and therefore the behavior of the free energy.

For the finite fluctuations D, we can also construct the non-equilibrium free energy as the form $\mathcal{F} = \mathcal{E} - D\mathcal{S} = \int DU P\, d\mathbf{x} - D[-\int P\ln P\, d\mathbf{x}] = D[\int P\ln(P/P_{ss})\, d\mathbf{x} - \ln Z]$, which is also a Lyapunov function and at non-equilibrium steady state, the non-equilibrium free energy becomes $\mathcal{F}_{ss} = \mathcal{E}_{ss} - D\mathcal{S}_{ss} = \int DU P_{ss}d\mathbf{x} - D[-\int P_{ss}\ln P_{ss}d\mathbf{x}] = -D\ln Z$. Here the partition function Z is defined as the form $Z = \int \exp(-U)d\mathbf{x}$ which is related to the population potential U.

III. THE EVOLUTIONARY DYNAMICS

Evolution theory is based on three fundamental principles: reproduction, mutation, and natural selection. The mathematical framework of evolutionary theory is based on describing the change in allele frequencies.[24–26] Allele is one of the multiple forms of a gene located at a specific position on a chromosome. The specific position is called locus. Most of higher eukaryotes are diploid, having two copies of each gene. In sexual reproduction, only one allele is transmitted into a single gamete, and two gametes unite to restore the double complement of alleles.

We consider here a single diploid locus with multiple alleles in a randomly mating diploid population. We denote the n alleles at the given locus by $A_1, A_2, \ldots, A_n$ and their frequencies by $x_1, x_2, \ldots, x_n$ ($\sum_i^n x_i = 1$), respectively. Due to the conservation of total allele frequencies, the n alleles system has $n-1$ degree of freedom and thus the state space is $n-1$ dimension: $\{x_k | 1 \le k \le n-1\}$.

A. Evolutionary driving force: Natural selection, mutation, genetic drift

1. Natural selection

"Survival of the fittest" is the common metaphor for the natural selection. Natural selection is expressed through the fitness which defined as the average number of offspring produced by individuals with a certain genotype. We can see how natural selection changes the allele frequencies by means of the fitness.

In a population consisted of N new born diploid individuals, there are total of x_ix_jN individuals with genotype A_iA_j. In the next generation, the expected number of offspring with genotype A_iA_j is $w_{ij}x_ix_jN$, and the expected total number of the population is $\sum_{ij}^n w_{ij}x_ix_jN$, where w_{ij} denotes the fitness of genotype A_iA_j. Then the proportion of A_i allele in the next generation will be $x_i' = \sum_j^n x_ix_jw_{ij}N/\sum_{ij}^n w_{ij}x_ix_jN = x_iw_i/\bar{w}$, where, $w_i = \sum_{j=1}^n x_jw_{ij}$ and $\bar{w} = \sum_{i=1}^n x_iw_i$. $\bar{w}$ is called mean fitness of population. Thus, the change rate of allele frequencies under natural selection is[24–26]

$$dx_i/dt = F_i^S = x_i(w_i - \bar{w})/\bar{w}. \tag{9}$$

Obviously, $\sum_{i=1}^n F_i^S = 0$.

2. Mutation

The process of replicating a gene is sometimes inaccurate. Mutation is the any change in the new gene from the parental gene. Obviously, mutation also results in the changes in allele frequency. The change rate of allele frequencies under mutation is[24–26]

$$dx_i/dt = F_i^M = \sum\nolimits_{j=1}^n x_jm_{ji} - x_i\sum\nolimits_{j=1}^n m_{ij}, \tag{10}$$

where, the m_{ji} is the rate per generation of mutation from allele A_j to A_i. Due to conservation of total frequency of alleles, $\sum_i^n x_i = 1$, we have $\sum_{i=1}^n F_i^M = 0$.

3. Genetic drift

Reproduction can be treated as a sampling process: a new generation with N individuals is formed as a sample of $2N$ alleles from a large pool of gametes. Due to the sampling nature of the reproduction, the allele frequencies are changed randomly. The change in allele frequencies resulting from the random process is called genetic drift which is a stochastic evolution force. The common mathematical approaches to deal with genetic drift is the diffusion approximation:[24–26]

$$\partial P/\partial t = D\nabla\cdot\nabla\cdot(\mathbf{G}P), \tag{11}$$

where $G_{ij} = x_i(\delta_{ij} - x_j)$ (note that the state space is $n-1$ dimension and thus $1 \le i, j \le n-1$) comes from the sampling nature of the genetic drift and $D = 1/(4N_e)$, N_e is the effective population size.

The matrix G_{ij} has some special properties. The first is

$$(\nabla\cdot\mathbf{G})_i = 1 - nx_i, \tag{12}$$

and the second is its inverse matrix is known to have the property:[25]

$$(\mathbf{G}^{-1}\cdot\mathbf{F})_i = F_i/x_i - F_n/x_n, \tag{13}$$

where $F_n = -\sum_{i=1}^{n-1} F_i$.

B. Mean fitness as the adaptive landscape for the frequency independent selection systems

If fitness of every genotype is not dependent on the frequency distribution of alleles, the corresponding natural selection is called frequency-independent selection. From

Eq. (9), the frequency-independent selection can be written as $\mathbf{F}^S = (1/2)\,\mathbf{G}\cdot\nabla \ln\bar{w}$, and thus $\nabla\times(\mathbf{G}^{-1}\cdot\mathbf{F}^S)=0$. Furthermore, $\nabla\times[\mathbf{G}^{-1}\cdot(\nabla\cdot\mathbf{G})]=\nabla\times[\nabla(\sum_{i=1}^{n}\ln x_i)]=0$. From Eq. (2), we can obtain $\mathbf{J}_{ss}=0$ for the population system with natural selection and genetic drift. In this case, $\mathbf{F}^S - D\nabla\cdot\mathbf{G} + D\mathbf{G}\cdot\nabla U = (1/2)\,\mathbf{G}\cdot\nabla\ln\bar{w} - D\nabla\cdot\mathbf{G} + D\mathbf{G}\cdot\nabla U = 0$. So, $\nabla\phi_0 = \nabla(DU)|_{D\to 0} = -(1/2)\nabla\ln\bar{w}$. Thus, we obtain

$$\phi_0 = -(1/2)\ln\bar{w} \tag{14}$$

for the frequency-independent selection population (here, we ignore the constant of integration).

According to the previous discussion, we can obtain $d\bar{w}/dt = \mathbf{F}\cdot\nabla\bar{w} = -2\bar{w}\mathbf{F}\cdot\nabla\phi_0 = 2\bar{w}\nabla\phi_0\cdot\mathbf{G}\cdot\nabla\phi_0 \geq 0$. The mean fitness as a Lyapunov function can be used to indicate where the evolutionary optima are. This picture is the Wright's adaptive fitness landscape with gradient nature. But, the Wright's adaptive fitness landscape will break down for the more general case, i.e., frequency-dependent selection.

C. The adaptive landscape for the general evolutionary dynamics

As mentioned, Wright's fitness landscape is inadequate for the general evolution dynamics such as frequency dependent selection. Then is there an adaptive landscape for evolution and if so what is it? Our potential-flux landscape theory provides a solution for this.

We can construct a Fokker-Planck equation including the selection, mutation, and genetic drift,

$$\partial P/\partial t = -\nabla\cdot[(\mathbf{F}^S+\mathbf{F}^M)P - D\nabla\cdot(\mathbf{G}P)]. \tag{15}$$

The corresponding steady state probability flux is $\mathbf{J}_{ss} = (\mathbf{F}^S+\mathbf{F}^M)P_{ss} - D\nabla\cdot(\mathbf{G}P_{ss}) = P_{ss}[(\mathbf{F}^S+\mathbf{F}^M - D\nabla\cdot\mathbf{G}) + D\mathbf{G}\cdot\nabla U]$.

The non-equilibrium intrinsic potential ϕ_0 of this system satisfies

$$(\mathbf{F}^S+\mathbf{F}^M)\cdot\nabla\phi_0 + \nabla\phi_0\cdot\mathbf{G}\cdot\nabla\phi_0 = 0. \tag{16}$$

Obviously ϕ_0 is a Lyapunov function always searching for optimum irrespective to whether the evolution system is in detailed balance or not. Therefore, ϕ_0 defines the true adaptive landscape for evolution.

D. Analogy between evolutionary dynamics and chemical reactions

It might be helpful for the chemistry and physics oriented readers to think about the analogy between evolutionary dynamics and chemical reactions to understand better the evolution dynamics, although we must point out such analogy is not exact and complete. For example, different alleles correspond to different chemicals, allele frequencies correspond to concentrations of different chemicals, birth and death correspond to birth and death of chemicals, mutation corresponds to chemical transformation, the genetic drift corresponds to the fluctuation in chemical reaction, etc. Furthermore, the allele frequency independent evolution corresponds to the chemical reactions with detailed balance, while the allele frequency dependent evolution corresponds to the chemical reactions without detailed balance. A good example is that the limit cycle can exist in both evolution and chemical reactions as a result of allele frequency dependent evolution and detailed balance breaking. In Eigen's proposed evolution theory, the analogy is even made more explicit. His hypercycle chemical reaction based equation is a replicator-mutator equation.[33] The evolutionary system with natural selection and mutation can also be described by such a replicator-mutator equation.[34]

IV. POTENTIAL AND FLUX LANDSCAPES AND NON-EQUILIBRIUM THERMODYNAMICS OF EVOLUTION

For the study of the general evolution dynamics, we consider the case of frequency dependent selection where the fitness is dependent on the allele frequency mimicking social interactions. We explore a group-help model (GHM) to study evolution dynamics including biotic interactions of individuals within a species.

A. Group-help model with frequency dependent selection for evolution

The frequency-dependent selection occurs when the fitness is dependent on the allele frequency distribution. The society is a typical frequency-dependent selection system. If the genotypes differ in their social behavior, the fitness of a genotype may depend on the composition of the population. For selection, we construct a GHM to explore the effect of interactions among individuals on the evolution.

We assume that a single diploid locus has three alleles A_1, A_2, A_3 with frequencies x_1, x_2, x_3, respectively. We take the fitness of the genotypes as follows:

$$\begin{aligned} w_{11} &= \alpha + 2\beta x_1x_2, & w_{12} &= \alpha + x_1x_1, & w_{13} &= \alpha + x_3x_3,\\ w_{21} &= \alpha + x_1x_1, & w_{22} &= \alpha + 2\beta x_2x_3, & w_{23} &= \alpha + x_2x_2,\\ w_{31} &= \alpha + x_3x_3, & w_{32} &= \alpha + x_2x_2, & w_{33} &= \alpha + 2\beta x_3x_1. \end{aligned} \tag{17}$$

Due to conservation of total allele frequency, we take $x_3 = 1 - x_1 - x_2$. The fitness of each genotype includes two components influenced by external physical environment (which is described by the parameter α) and biotic interactions characterized by strength β.

The scheme of the group help model with frequency dependent selection for evolution is shown in Fig. 1(a). In this random mating population, three groups are formed and two genotype members help each other within each group. This can be due to kin selection which shows the one's

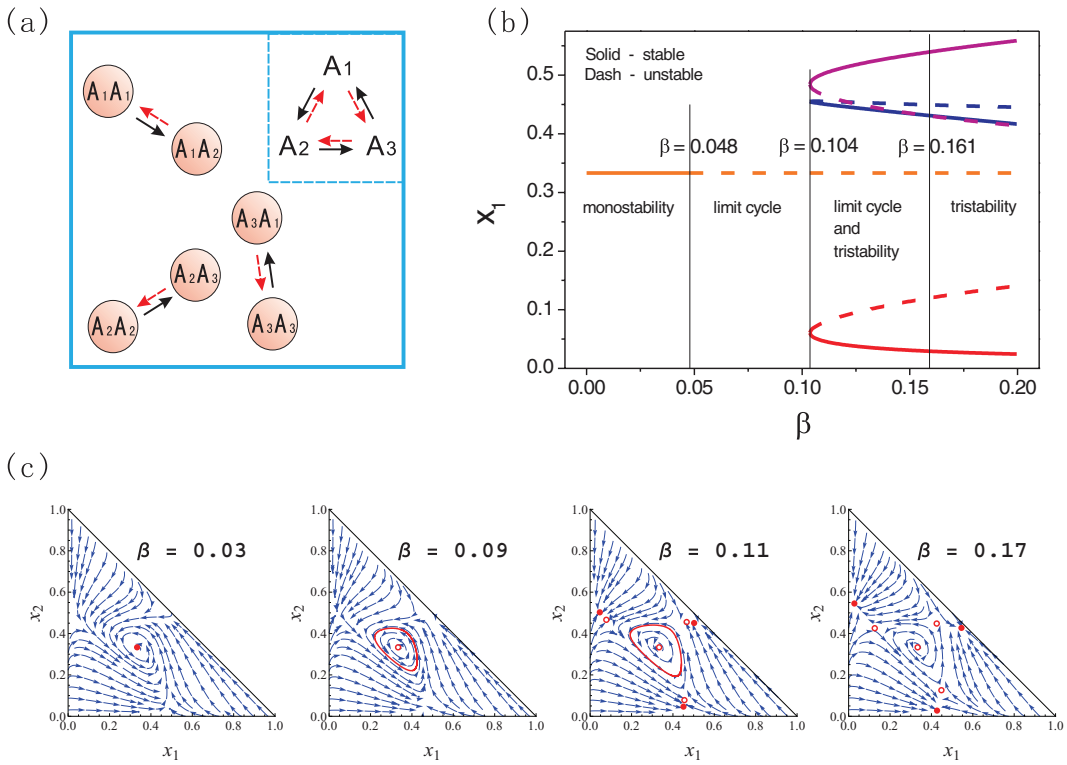

FIG. 1. Scheme for group-help model and the phase diagrams. (a) The scheme of the group-help model. (b) The change of phase of the group-help model with the assistance factor β. (c) The streamlined figure (monostability phase at $\beta = 0.03$, limit cycle phase at $\beta = 0.09$, limit cycle and tristability coexisting phase at $\beta = 0.11$, tristability phase at $\beta = 0.17$).

relatives (who carry many of the same genes) help it to survive and reproduce. The heterozygote helps the homozygote with the assistance factor $\beta(\beta \geq 0)$, while the homozygote helps the heterozygote with the constant assistance factor 1. We can obtain a frequency-dependent selection force via inserting these fitness (Eq. (17)) into Eq. (9). This selection has $\nabla \times (\mathbf{G}^{-1} \cdot \mathbf{F}^S) \neq 0$. It will induce a non-zero steady state probability flux, $\mathbf{J}_{ss} \neq 0$, breaking the detailed balance.

Here, we give a biological description for understanding this selection model. Due to symmetry, the equally coexisting state, $x_1 = x_2 = x_3 = 1/3$, is a steady state. From $F_i^S = x_i(w_i - \bar{w})/\bar{w}$, we can see the same component α can only influence the evolutionary speed not the evolutionary direction (one can check that α term contribution does not come in the numerator but only through the denominator of the selection force). We temporarily take $\alpha = 0$ which is useful to explore the evolutionary direction. Due to random mating, we expect that the heterozygote tends towards equally coexisting of all the alleles and the homozygote tends towards excluding other types of alleles. For convenience, we define a function $k(i)$ in the form: $k(1) = 2$, $k(2) = 3$, $k(3) = 1$. When the assistance factor $\beta = 0$, there is only black solid arrows coming from assistance of homozygote to heterozygote (Fig. 1(a)). In this case, the homozygote cannot survive to the reproductive age due to low fitness so that the reproduction is done by heterozygote. But the homozygote A_iA_i is also generated by random mating and helps the heterozygote $A_iA_{k(i)}$ to survive. Thus, the allele A_i will benefit survival of $A_{k(i)}$. If the population deviates from the equally coexisting state, an oscillation occurs by flowing along the direction $A_1 \to A_2 \to A_3 \to A_1$ and finally settles back to the equally coexisting state. On the contrary, when $\beta \to \infty$, the reproduction is done by homozygote due to the low fitness of heterozygote. We can simply think there is only red dashed arrows (Fig. 1(a)) in this case coming from assistance from heterozygote to homozygote. The heterozygote $A_iA_{k(i)}$ is also generated by random mating and helps the homozygote A_iA_i to survive. Thus, the allele $A_{k(i)}$ will benefit survival of A_i. If the population slightly deviates the equally coexisting state, an oscillation also occurs by flowing along the direction $A_1 \to A_3 \to A_2 \to A_1$ and finally settles to a state in which the population is predominated by an allele. We can easily see there are three such states correspond to the three alleles, respectively. The effect of β is to adjust the weights of the two arrows denoted by black solid and red dashed.

Besides the selection, we take into account the mutation as the form Eq. (10) to prevent the gene loss. In the following detailed calculation, the α and the mutation rate are taken as constant: $\alpha = 0.1$ and $m_{ij} = 0.01$ for any i and j. This simple type of mutation force also tends towards equally coexisting of all the alleles. We change the assistance factor β to explore its effect on the evolution. Figure 1(b) shows the change of the frequency of the allele A_1 under different assistance factor β. The system has four phase regions with parameter β increasing: mono-stability phase, a limit cycle oscillation phase, a limit cycle oscillation and tri-stability coexisting phase, tristability phase. Figure 1(c) shows the streamlines for the case of $\beta = 0.03, 0.09, 0.11, 0.14$. The hollow dots represent the unstable points while the solid dots represent the stable points. In the case of $\beta = 0.09$ and $\beta = 0.11$, the red solid circles are the limit cycle. When $0 \leq \beta \leq 0.048$, the evolutionary dynamics is mainly dominated by the mutation which tends towards

the equally coexisting of all the alleles. The state, $x_1 = x_2 = x_3 = 1/3$, is a global stable state. We can see one stable point exist for the case of $\beta = 0.03$ in Fig. 1(c). For $\beta > 0.048$, the effect of selection exceeds the mutation to dominate the evolutionary dynamics. When $0.048 < \beta < 0.104$, the selection is predominated by the assistance from homozygote to the heterozygote denoted by the black solid arrows. We can see a stable limit cycle with the oscillation direction, $A_1 \to A_2 \to A_3 \to A_1$, for case of $\beta = 0.09$ in Fig. 1(c). When the assistance factor slightly increases to $0.104 < \beta < 0.161$, the effect of assistance from heterozygote to the homozygote denoted by the red dashed arrows begins to emerge. For the case of $\beta = 0.11$ in Fig. 1(c), three stable steady states emerge around the limit cycle. From the locations of the stable states, we can see the survival of a particular allele can be preserved while at the same time the others restrained, but they do not get completely lost due to the mutation (stable points do not sit exactly at the axis or the vertex node in Fig. 1(c)). When $\beta \geq 0.161$, the limit cycle is destroyed by the increased effect of the assistance from heterozygote to the homozygote (the case of $\beta = 0.17$ in Fig. 1(c)). The population will stay at one of the three stable states. The stable states are close to the vertexes of triangle with further increasing of β. We saw for all the case in Fig. 1(c), the rotating direction is counterclockwise $A_1 \to A_2 \to A_3 \to A_1$. When $\beta > 2$, the selection is predominated by the assistance from heterozygote to the homozygote denoted by the red dashed arrows. Consequently, the rotating direction will be changed to the clockwise $A_1 \to A_3 \to A_2 \to A_1$.

B. The underlying potential-flux landscapes for the general evolutionary dynamics

Wright's adaptive fitness landscape with gradient nature is invalid for the general case, for example, frequency-dependent selection population system. This can be easily proved by a simple case. For instance, the frequency-dependent selection can induce a limit cycle type evolution. The change of fitness is not monotonous along the limit cycle. Our potential-flux landscape provides a way of obtaining the true adaptive landscape for evolution. Here, we construct the Lyapunov function ϕ_0 to quantify the true intrinsic adaptive landscape. We also consider the population landscape U for the finite population with fluctuations.

Now, we will discuss the four phases under different parameters: the mono-stability phase, $\beta = 0.03$; a limit cycle phase, $\beta = 0.09$; coexistence of a limit cycle and tri-stability phase, $\beta = 0.11$; the tri-stability phase, $\beta = 0.17$. The fluctuation strength is taken as $D = 3 \times 10^{-4}$, when obtaining the population potential $U = -\ln P_{ss}$.

To obtain the intrinsic and population potential landscape as well as the corresponding flux for the group-help model for evolution dynamics, we need to solve the corresponding Fokker-Planck equation (Eq. (15)) for $U = -\ln P_{ss}$ where P_{ss} is the steady state probability, and Hamilton-Jacobi equation (Eq. (16)) for ϕ_0. We take the zero flux boundary condition, $\mathbf{n} \cdot \mathbf{J}_{ss} = \mathbf{n} \cdot [(\mathbf{F}^S + \mathbf{F}^M)P - D\nabla \cdot (\mathbf{G}P)] = 0$, for the Fokker-Planck equation (Eq. (15)). The $\mathbf{n}$ denote the unit normal vector of boundary. Such condition corresponds to the conservation of total probability. We obtain the numerical solution of the steady state Fokker-Planck equation P_{ss} and the associated population potential U. Correspondingly, the boundary condition of Hamilton-Jacobi equation (Eq. (16)) is taken as the form $\mathbf{n} \cdot (\mathbf{F}^S + \mathbf{F}^M + \mathbf{G} \cdot \nabla\phi_0) = 0$, which is the zero-fluctuation limit of the zero flux boundary condition. The Hamilton-Jacobi equation is impossible to solve exactly with an analytic solution and also challenging to get the numerical solution. The notion of viscosity solution was introduced to solve the Hamilton-Jacobi equation. According to this notion, a numerical method – level set method was devised and developed. In this paper, we use the Mitchell's level-set toolbox to solve the Hamilton-Jacobi equation for intrinsic potential ϕ_0.[35]

Figure 2 shows the population potential U(the top row) and intrinsic potential ϕ_0 (the bottom row), respectively. The arrows on the landscape in Fig. 2 are schematic to describe the two component of driving force: negative gradient of the landscape ($-\nabla U$ for top row and $-\nabla\phi_0$ for bottom row)(black arrows) and the steady state probability flux ($\mathbf{J}_{ss}/P_{ss}$ for top row and intrinsic flux velocity $\mathbf{V} = (\mathbf{J}_{ss}/P_{ss})_{D\to 0}$ for bottom row)(purple arrows). The arrows at the bottom of each subfigure are the projection of the direction of those arrows. The flux (purple arrows) and negative gradient of U (black arrows) are almost perpendicular to each other on the bottom plane of Figs. 2(a)– 2(d). We can see the flux $\mathbf{J}_{ss}/P_{ss}$ (purple arrows) and negative gradient of ϕ_0 (black arrows) are perpendicular to each other on the bottom plane of Figs. 2(e)–2(h). The non-equilibrium intrinsic potential landscape ϕ_0 does not change with fluctuation strength D. The effect of D on the probability is through the $-\ln P_{ss} = U \cong \phi_0/D$ under weak fluctuations.

Figures 2(a) and 2(e) show the U and ϕ_0 for the case of the mono-stable state ($\beta = 0.03$). While the negative gradient of potential (black arrows) attracts the system into the minimum of the funnel (basin of attractions), the flux around the basin is driven by the intrinsic flux velocity (purple arrows). Without the former, the system will not be attracted to the bottom of the attractor basin or funnel. Without the latter, the system will go straightly down to the low potential basin. The effect of the intrinsic flux becomes more important when the system spirally approaches to the bottom of the basin. It is interesting to notice that the intrinsic potential ϕ_0 gives the essential topography (funnel) of the landscape for global stability.

Figures 2(b) and 2(f) show the U and ϕ_0 for the case of one limit cycle ($\beta = 0.09$). Under finite fluctuations, the system is at limit cycle oscillation phase with the topography of the landscape as a Mexican hat shape with a closed ring valley for oscillations. The forces from negative gradient of the potential are nearly negligible along the closed ring and more significant inside and outside ring. So, away from the closed ring, the evolution is attracted by the negative landscape gradient towards the closed ring. On the Mexican hat closed ring valley, the flux dominates the negative gradient of the potential landscape and is the driving force for coherent oscillation. The direction of the flux near the ring is parallel to the oscillation path. This is much like a water flow moving through a channel. We can also see the underlying intrinsic landscape ϕ_0 has a Mexican hat like topography with constant ϕ_0 values along the oscillation ring valley (U is not

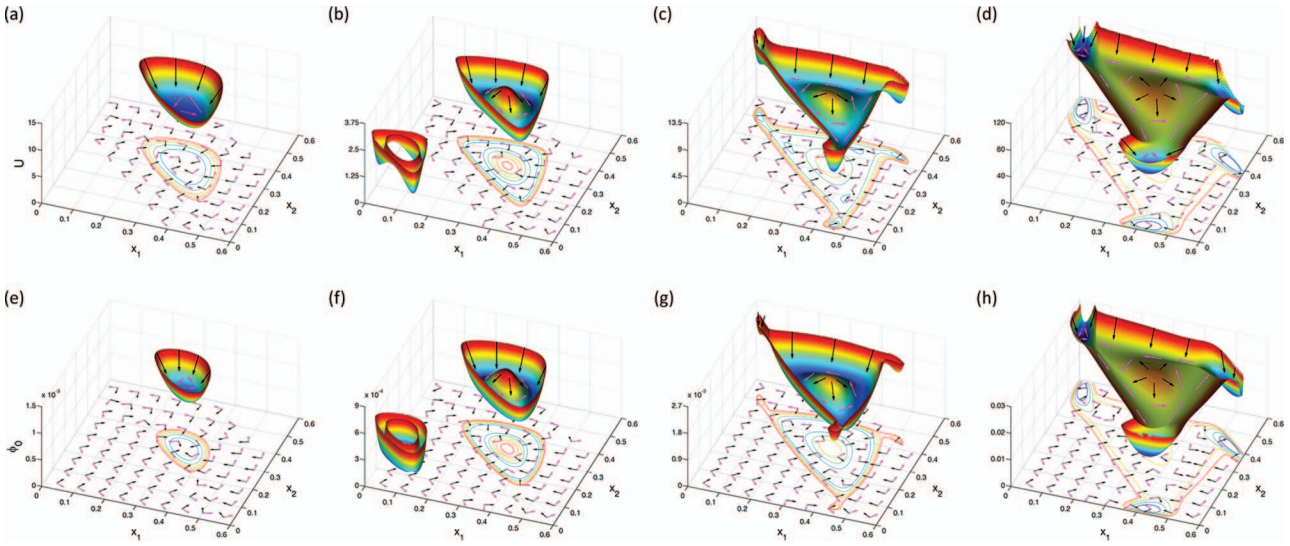

FIG. 2. Potential and flux landscapes of different phases. Top row: The population potential landscape U and the steady state probability flux $\mathbf{J}_{ss}$ ((a): $\beta = 0.03$ for monostability phase. (b): $\beta = 0.09$ for limit cycle phase. (c): $\beta = 0.11$ for limit cycle and tristability coexisting phase. (d): $\beta = 0.17$ for tristability phase). In (b), the lower left corner sub-picture shows the enlarged (U is enlarged by 5 times) valley bottom of the population potential landscape. The arrows on the surface are schematic to describe the two component of driving force: negative gradient of the population potential landscape $-\nabla U$ (by black arrows) and the steady state probability flux $\mathbf{J}_{ss}$ (by purple arrows). The arrows at the bottom of each subfigure are the projection of the direction of those arrows: the black arrows represent $-\nabla U$ and the purple arrows represent $\mathbf{J}_{ss}$. Bottom row: The adaptive landscape defined by intrinsic potential ϕ_0 and the intrinsic flux velocity $\mathbf{V} = (\mathbf{J}_{ss}/P_{ss})_{D\to 0}$ ((e): $\beta = 0.03$ for monostability phase. (f): $\beta = 0.09$ for limit cycle phase. (g): $\beta = 0.11$ for limit cycle and tristability coexisting phase. (h): $\beta = 0.17$ for tristability phase). In (f), the lower left corner sub-picture shows the enlarged(ϕ_0 is enlarged by 6 times) valley bottom of the intrinsic potential landscape. The arrows on the surface are schematic to describe the two component of driving force: negative gradient of the intrinsic potential landscape $-\nabla\phi_0$ (by black arrows) and the intrinsic flux velocity $\mathbf{V}$ (by purple arrows). The arrows at the bottom of each subfigure are the projection of the direction of those arrows: the black arrows represent $-\nabla\phi_0$ and the purple arrows represent $\mathbf{V}$.

constant along the ring since U is a direct reflection of steady state probability $U = -\ln P_{ss}$. U is not a Lyapunov function in general but captures more details than ϕ_0, i.e., the inhomogeneity of the steady probability due to the inhomogeneous speed on the ring). The non-equilibrium intrinsic potential ϕ_0 being Lyapunov function essentially characterizes the global topography of the oscillation landscape.

Figures 2(c) and 2(g) show the U and ϕ_0 for the case of coexistence of a limit cycle oscillation and tri-stability phase ($\beta = 0.11$). The topography of the landscape looks like three basins around a Mexican hat ring valley. We can see the steady state probability flux on the closed ring valley landscape of the limit cycle is more significant than that of the negative gradient of the potential landscape, therefore driving the coherent oscillations, but less significant compared with gradient force around the three stable basins of attraction. The direction of the flux near the ring is parallel to the oscillation path and curling around near the bottom of the three stable basins of attraction. The forces from negative gradient of the potential landscape are nearly negligible on the closed ring. They are significant away from the oscillation ring and the bottom of the three basin valleys. So away from the closed ring and the bottom of the three basins of attraction, the evolution is attracted by the landscape towards the closed ring and three basins of attractions. We noticed the constant ϕ_0 on the limit cycle oscillation ring.

Figures 2(d) and 2(h) show the U and ϕ_0 for the case of the tri-stability phase ($\beta = 0.17$). We can see three basins of attraction clearly with equal depths due to the symmetry. The direction of the flux near the linking region between the two attractors is parallel to the link. The directions of the flux are curling around the bottom of three basins of attractions. The forces from negative gradient of the potential landscape are less significant along the links between the two attractors (away from the attractors) and more significant near the basins of attractions. So near the basins of attractions, the evolution is attracted by the landscape towards the basin. Along the links between the attractors, the dynamics of the evolution is mainly driven by the intrinsic flux.

C. Quantitative criterion for stability and robustness of evolution against fluctuations

For the mono-stable case, we define robustness ratio as $\Lambda = \delta U/\Delta U$. The gap $\delta U = \langle U\rangle - U_m$ is the difference between the average of $\langle U\rangle = \int(-\ln P_{ss})P_{ss}d\mathbf{x}$ and the global minimum $U_m = \min[U(\mathbf{x})]$. The δU is a measure of the bias or the slope towards the global minimum of the potential landscape. The ΔU is defined as $\Delta U = (\langle U^2\rangle - \langle U\rangle^2)^{1/2}$ which is a measure of the averaged roughness (fluctuations) or the local trapping of the potential landscape. Figure 3(a) shows the change of global maximum probability $P_{max} = \exp(-U_m)$ (at the bottom of basin of attraction) with respect to Λ as fluctuation strength characterized by diffusion D changes. It implies that the system is more stable and robust (stable against changes) when the fluctuations are small. It also shows that when the bias or the slope against roughness Λ is large, the system is more stable and more likely to stay at the bottom of the basin of attraction.

For limit cycle case, once we have the potential landscape, we can discuss the global stability and robustness of the evolution from the barrier heights escaping from the

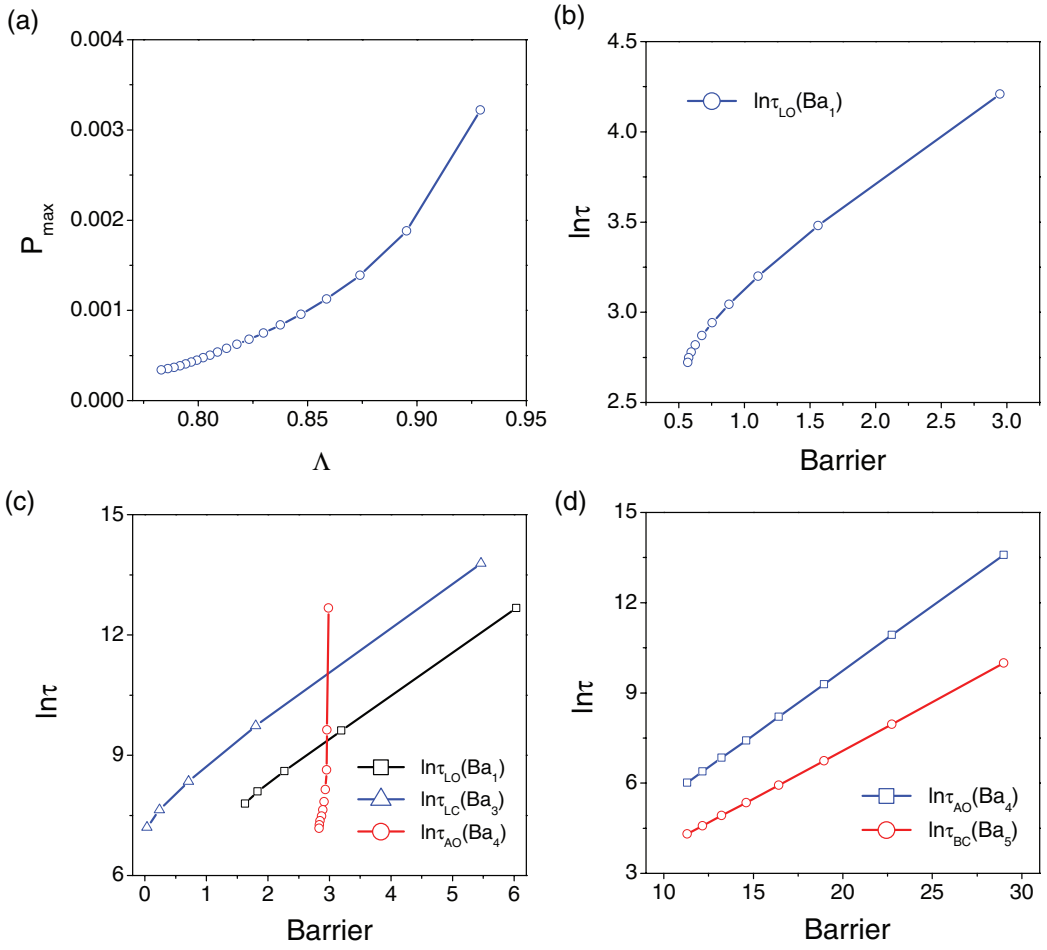

FIG. 3. Landscape topography, kinetic time and global stability against fluctuations. (a) The maximum of probability P_{max} versus the parameter Λ for $\beta = 0.03$. (b) The MFPT versus the *barrier* for $\beta = 0.09$. τ_{AB} means the transition time from state A to state B. L is population potential minimum point along the limit cycle and O is the population potential maximum point inside the limit cycle circle (the top of the Mexican hat). (c) The MFPT versus the *barrier* for $\beta = 0.11$, $Ba_3 = U_{Saddle1} - U_L$, $Ba_4 = U_O - U_S$, $Ba_5 = U_{Saddle2} - U_S$. $U_{Saddle1}$ is the potential at the saddle point between the stable state and limit cycle, U_S is the potential minimum in the one of three stable states, $U_{Saddle2}$ is the population potential at the saddle point between the two stable states. The locations of A, B, and C are shown in Fig. 6. (d) The MFPT versus the *barrier* for $\beta = 0.17$.

attractor region. The barrier height is a measure of transition from the limit cycle attractor to outside. We define the barrier heights as: $Ba_1 = U_O - U_L$, where, U_L is the potential minimum along the limit cycle and U_O is the potential at the local maximum point inside the limit cycle circle (the top of the Mexican hat).

The stability is related to the escape time from the basins of attraction. Since the evolution is characterized by the basins of attractions with large weights, the easier it is to escape and the more communications between the states, the less stable the system is. For the probabilistic description of the evolution dynamics above with diffusion equation, the mean first-passage time (MFPT) for escape time $\tau(\mathbf{x})$ starting from a state $\mathbf{x}$ obeys:[31] $\mathbf{F} \cdot \nabla\tau + D\,\nabla\tau \cdot \mathbf{D} \cdot \nabla\tau = -1$ (details in Appendixes). It is essentially the average time it takes from an initial position to reach a given final position.

Figure 3(b) shows the escape time from the basin of oscillation ring increases, when the associated barrier height increases. The barrier height increases as the fluctuations decrease. Then, the limit cycle attractor becomes more stable, since it is harder to go from the ring to outside. So, small fluctuations and large barrier heights serve as the source for the robustness and stability of the evolutionary system. In other words, it is less likely for the system to change from its limit cycle attractor and destroy the coherence (details in Appendixes). The system becomes robust. This is an illustration of how evolutional robustness is realized for the oscillation network.

Figure 3(c) shows the escape time increases, when the associated barrier heights of limit cycle and the stable states are higher as the fluctuations decrease. Then, the limit cycle attractor and three stable states become more robust and stable, since it is harder to go from the ring and the valleys to outside.

Figure 3(d) shows the escape time increases when the associated barrier heights of escaping from the stable state are higher as the fluctuations decrease. Then, the stable state attractors become more robust and stable, since it is harder to go from the inside of attractor to the outside or communicate to outside.

From Figures 3(b), 3(c), and 3(d), we see a nearly linear relationship between $\ln\tau$ and *Barrier*. This implies that the escape time scale from a basin of attraction is exponentially related to the barrier height, i.e., $\tau \sim \exp(-Barrier)$. We see population landscape topography through barrier heights

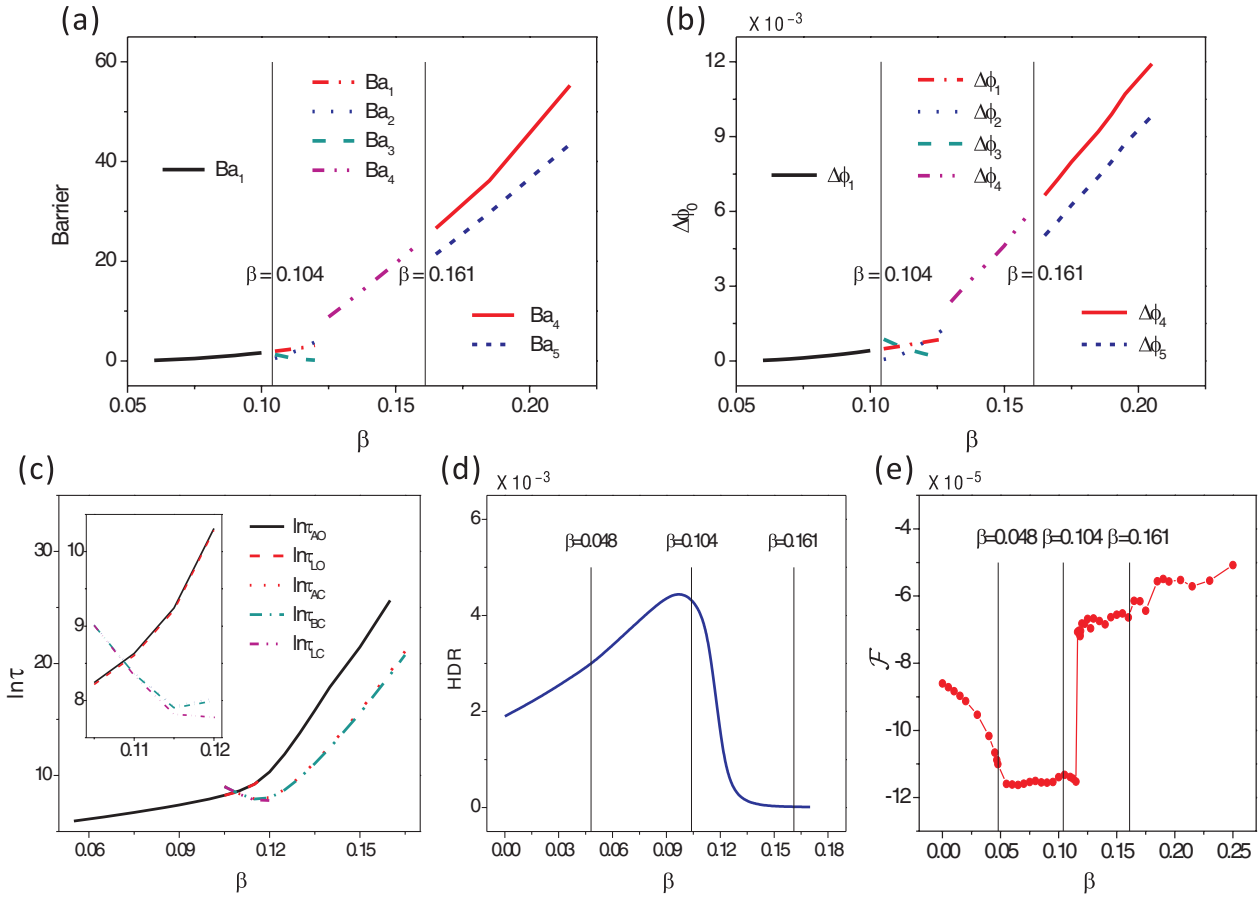

FIG. 4. Landscape topography, kinetic time and global stability versus biotic interactions. (a) The barrier heights from the population potential landscape versus β. (b) The barrier heights from the intrinsic potential landscape versus β. $\Delta\phi_1 = \phi_{0O} - \phi_{0L}$, $\Delta\phi_2 = \phi_{0Saddle1} - \phi_{0S}$, $\Delta\phi_3 = \phi_{0Saddle1} - \phi_{0L}$, $\Delta\phi_4 = \phi_{0O} - \phi_{0S}$, $\Delta\phi_5 = \phi_{0Saddle2} - \phi_{0S}$. ϕ_{0L} is the intrinsic potential minimum along the limit cycle attractor. ϕ_{0O} is the intrinsic potential at the local maximum point inside the limit cycle circle, $\phi_{0Saddle1}$ is the intrinsic potential at the saddle point between the stable state and limit cycle. ϕ_{0S} is the intrinsic potential minimum in the one of three stable state attractors. $\phi_{0Saddle2}$ is the intrinsic potential at the saddle point between the two stable states. (c) The MFPT versus β. (d) The HDR versus β. (e) The intrinsic free energy versus β.

provides quantitative criterions for the global stability and robustness.

D. Quantitative criterions for global stability and robustness of evolution versus biotic interactions

We explore how the parameter β changes the stability and robustness of the evolution dynamics.

Figures 4(a) and 4(b) show that the barrier heights from population potential landscape (U) and intrinsic potential landscape (ϕ_0) increase as the parameter β increases. Since barrier height is a quantitative measure of how difficult it is to go from one part of the state space to the other, the higher the barrier, the harder it is to communicate from one place to another. The system will be more stable if the states are not easily changed from one to the other. This implies the system becomes more stable and robust when β increases. From Figures 4(b) and 4(c), we can also derive a nearly linear relationship between $\ln\tau$ and the barrier height of the intrinsic potential landscape $\Delta\phi_0$. So the escape time is exponentially related to the barrier height: $\tau \sim \exp(-\Delta\phi_0)$. This illustrates that the landscape topography through the barrier heights can characterize the global stability of the evolution.

Figure 4(c) shows the MFPT varies with the parameter β, we can see it is closely correlated with the barrier height. As barrier height increases, MFPT increases. So the potential landscape topography through barrier height is a good measure of the kinetics and the communications between the states of the system. Therefore, it can be used to quantify the global stability of the system.

Figure 4(d) shows the steady state heat dissipation rate (HDR $= \int d\mathbf{x}[\mathbf{J}_{ss} \cdot \mathbf{G}^{-1} \cdot (\mathbf{F} - D\nabla \cdot \mathbf{G})]$) increases first then decreases as β increases. This implies the system from monostability to limit cycle oscillations might consume more of the energy to maintain the coherence. Therefore, the system dissipates more. On the other hand, as β increases, the system experiences a transition from limit cycle oscillations to the three stable basins of attractions. Therefore, as coherence structure of limit cycle is disappearing, the dissipation will be less.

E. The non-equilibrium global phases and phase transitions of evolution from intrinsic free energy

As discussed earlier, in the equilibrium system, once the free energy of the system is known, the global physical properties of thermodynamics for the system can be explored. So, to obtain information on these quantities is very important for both equilibrium system and non-equilibrium system. Here we will use our proposed method described earlier in

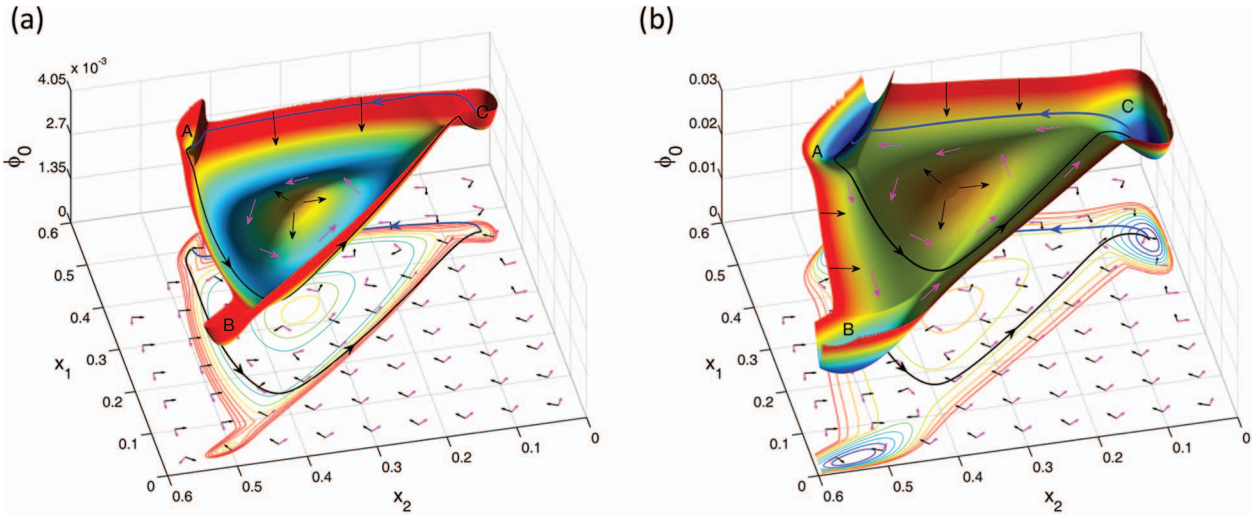

FIG. 5. The evolutionary pathways on the intrinsic potential landscape ϕ_0. ((a): $\beta = 0.11$ for limit cycle and tristability coexisting phase. (b): $\beta = 0.17$ for tristability phase.)

this paper to obtain the non-equilibrium free energy for the three allele evolution. Figure 4(e) shows the intrinsic free energy versus the parameter β with the small fluctuation $D = 1 \times 10^{-5}$. We can see clearly that the intrinsic free energy goes down smoothly when $0 \leq \beta \leq 0.048$. There are two phase transition points: $\beta = 0.048$ and $\beta = 0.116$. Although the non-equilibrium intrinsic free energy is continuous in parameter β, the slope (first derivative) of the non-equilibrium intrinsic free energy is discontinuous at the two points. Analogous to equilibrium statistical mechanics, this is a signal of thermodynamic phase transition. At $\beta = 0.048$, the system transforms from mono-stability phase to limit cycle oscillation phase. The limit cycle oscillation and tri-stability phase coexist near $\beta = 0.116$. But, the topology of state space transforms from the domination of limit cycle to the domination of tri-stable state. We can see here for non-equilibrium evolution system our constructed non-equilibrium free energy can reflect the global phases of the underlying dynamical system as well as the associated phase transitions. Therefore, we can use this non-equilibrium free energy function to explore the global stability of the evolutionary dynamics.

F. Quantifying the evolution pathways

Quantifying biological pathway is critical in uncovering the evolutionary dynamical process and the underlying mechanisms. We now quantify the dynamics and the path probability of starting from initial configuration $\mathbf{x}_i$ at $t = 0$ and end at the final configuration of $\mathbf{x}_f$ at time t, with a path integral representation[36,37] as $P(\mathbf{x}_f, t \mid \mathbf{x}_i, 0) = \int D\mathbf{x} \exp(-\int L(\mathbf{x}(t))dt)$, where $L = (1/4)D^{-1}\dot{\mathbf{x}} \cdot \mathbf{D}^{-1} \cdot \dot{\mathbf{x}} - (1/2)D^{-1}\mathbf{F} \cdot \mathbf{D}^{-1} \cdot \dot{\mathbf{x}} + V$ is the Lagrangian of the system and $V = (1/4)D^{-1}\mathbf{F} \cdot \mathbf{D}^{-1} \cdot \mathbf{F} + (1/2)\mathbf{D} \cdot \nabla \cdot (\mathbf{D}^{-1} \cdot \mathbf{F})$. In the zero fluctuation limit $D \to 0$, we have $V(\mathbf{x}) = (1/4)D^{-1}\mathbf{F} \cdot \mathbf{D}^{-1} \cdot \mathbf{F}$. The exponential factor gives the weight of each path. So the probability of evolution dynamics from initial configurations $\mathbf{x}_i$ to the final state $\mathbf{x}_f$ is equal to the sum of all the different weights over all possible paths $D\mathbf{x}$. Not every path contributes to the same weight. We can identify the dominant paths which give the most contribution to the weight.

Figures 5(a) ($\beta = 0.11$) and 5(b) ($\beta = 0.17$) show the dominant pathways by black line from basin A to basin C and from C to A by blue line in the zero fluctuation limit, $D \to 0$ (the case of finite fluctuation is given in the Appendixes). We can see clearly that evolution pathways do not follow the gradient paths on the underlying potential landscape. This results from the non-zero flux. The additional dynamical driving force from the flux leads to the deviations from the naively expected gradient paths. The dominant pathways may not necessarily pass the saddle point or transition state. This is very different from the equilibrium case where the dominant paths go through saddle point between the basins of attractions. Furthermore, the forward evolution pathways (A to C) and backward evolution pathways (C to A) are different. So, the evolution pathways are irreversible. The irreversibility is very fundamental and provides a new prediction to test for evolutionary biology.

V. GENERALIZING FISHER'S FUNDAMENTAL THEOREM OF NATURAL SELECTION

The validity of Wright's adaptive fitness landscape is guaranteed by Fisher's fundamental theorem of natural selection (FTNS) (Ref. 2) which is about the adaptive rate resulting from natural selection. The mathematical form in constant environments is given as follows:[38]

$$d\bar{w}/dt = V_A(w)/\bar{w}, \tag{18}$$

where, $V_A(w) = 2\sum_{i=1}^{n} x_i(w_i - \bar{w})^2$ is the additive genetic variance. So the change of the mean fitness is from the effects of selection favoring the most fit individuals among variations. Since the variance is always larger or equal to zero, Fisher's fundamental theorem implies mean fitness never decreases with constant environment. However, the mean fitness is not a Lyapunov function in general. The Fisher's FTNS and the Wright's mean fitness adaptive landscape hold in the frequency-independent case. In the early part of this

paper, we discussed the inadequacy of Wright's landscape and the possible resolution with our theory of potential and flux landscape. Now we have found that the intrinsic potential ϕ_0 is a Lyapunov function which can be used to define the adaptive landscape for general evolution dynamics. Then, how about the relationship between the adaptive rate and genetic variations in the general evolutionary dynamics? We will generalize the Fisher's FTNS with our potential-flux theory.

We consider more general case of an overall population system consists of N species interacting to each other. Here, we construct this system to include all the biotic interactions of individuals within a species or between species. We consider only natural selection takes effect and population size of all species is infinite (the effect of mutation will be studied elsewhere). If the ith species is sexual, it has n_i alleles at the given locus, $\mathbb{A}_1^{(i)}$, $\mathbb{A}_2^{(i)}$, $\ldots$, $\mathbb{A}_{n_i-1}^{(i)}$, $\mathbb{A}_{n_i}^{(i)}$, with frequency $\mathbb{X}_1^{(i)}$, $\mathbb{X}_2^{(i)}$, $\ldots$, $\mathbb{X}_{n_i-1}^{(i)}$, $1-\sum_{k=1}^{n_i-1}\mathbb{X}_k^{(i)}$, the fitness of genotype $\mathbb{A}_k^{(i)}\mathbb{A}_l^{(i)}$ is $w_{kl}^{(i)}$ and the marginal fitness of allele $\mathbb{A}_k^{(i)}$ is $w_k^{(i)}=\sum_{l=1}^{n_i}\mathbb{X}_l^{(i)}w_{kl}^{(i)}$. If the ith species is asexual, it has n_i genotypes at the given locus, $\mathbb{A}_1^{(i)}$, $\mathbb{A}_2^{(i)}$, $\ldots$, $\mathbb{A}_{n_i-1}^{(i)}$, $\mathbb{A}_{n_i}^{(i)}$, with frequency $\mathbb{X}_1^{(i)}$, $\mathbb{X}_2^{(i)}$, $\ldots$, $\mathbb{X}_{n_i-1}^{(i)}$, $1-\sum_{k=1}^{n_i-1}\mathbb{X}_k^{(i)}$, and the fitness of genotype $\mathbb{A}_k^{(i)}$ is $w_k^{(i)}$. We have a $\sum_{i=1}^{N}(n_i-1)$ dimensional overall space, in which the state of overall population is given by $\mathbb{X}$. The ith subspace $\{\mathbb{X}_k^{(i)}|1\le k\le n_i-1\}$ belongs to the ith species. The interactions between species are through the fitness. For instance, the influence of jth species to ith species is described by $w_{kl}^{(i)}(\cdots,\mathbb{X}^{(j)},\cdots)$ if ith species is sexual and by $w_k^{(i)}(\cdots,\mathbb{X}^{(j)},\cdots)$ if ith species is asexual. The natural selection can be written as $d\mathbb{X}_k^{(i)}/dt=\mathbb{F}_k^{(i)}=\epsilon^{(i)}\mathbb{X}_k^{(i)}[w_k^{(i)}-\bar{w}^{(i)}]/\bar{w}^{(i)}$ for either case of sexual or asexual ith species.[26] Due to different one-generation lengths for different species, we introduce the weight $\epsilon^{(i)}$ ($\epsilon^{(i)}>0$) to unify the evolutionary time for every species. For genetic drift, we use Wright-Fisher model (i.e., random mating process with non-overlapping generation) for sexual species and Moran model (i.e., birth-death process with overlapping generation) for asexual species.[24,25] The diffusion matrix of the overall population can be written as[25] $\mathbb{G}_{kl}^{(ij)}=\delta_{ij}\epsilon^{(i)}[\mathbb{X}_k^{(i)}(\delta_{kl}-\mathbb{X}_l^{(i)})]$, where δ_{ij} describes that there is no relationship between different species. We can see the matrix $\mathbb{G}$ is a block diagonal and a positive definite matrix.

If the fitness of every genotype is not dependent on any allele frequency of any species, we can also call the overall population frequency-independent selection population. In this case, the natural selection force takes the form: $\mathbb{F}=(1/2)\ \mathbb{G}\cdot\nabla[\sum_{i=1}^{N}(1+\delta^{(i)})\ln\bar{w}^{(i)}]$, where $\delta^{(i)}=0$ for sexual i-species and $\delta^{(i)}=1$ for asexual i-species. This is a simple composition of frequency-independent selection forces of all species. For this system, $\mathbb{V}(\mathbb{G})=0$, due to $\nabla\times(\mathbb{G}^{-1}\cdot\mathbb{F})=\nabla\times\{(1/2)\nabla[\sum_{i=1}^{N}(1+\delta^{(i)})\ln\bar{w}^{(i)}]\}=0$. We can obtain the intrinsic potential $\phi_0(\mathbb{G})=-(1/2)[\sum_{i=1}^{N}(1+\delta^{(i)})\ln\bar{w}^{(i)}]$.

If the fitness is dependent on allele frequency of species, the selection force does not have a simple gradient form as above in the independent case. As mentioned earlier in this work, we now can find the non-equilibrium intrinsic potential ϕ_0 as the general Lyapunov function to define the adaptive landscape and quantitatively describe the evolution dynamics. Accordingly, the adaptive rate of the population system can be measured by $d\phi_0/dt$ rather than fitness change rate. We will consider the general case for evolution dynamics and obtain the adaptive rate below. For any positive definite matrix $\mathbb{D}$, the general selection force can be decomposed to the intrinsic potential $\phi_0(\mathbb{D})$ and the corresponding intrinsic flux velocity $\mathbb{V}(\mathbb{D})$:

$$\mathbb{F}=-\mathbb{D}\cdot\nabla\phi_0+\mathbb{V}. \tag{19}$$

Since $\mathbb{V}\cdot\nabla\phi_0=0$, we get $\mathbb{F}\cdot\mathbb{D}^{-1}\cdot\mathbb{F}=\nabla\phi_0\cdot\mathbb{D}\cdot\nabla\phi_0+\mathbb{V}\cdot\mathbb{D}^{-1}\cdot\mathbb{V}$. Thus, the adaptive rate can be given by

$$\begin{aligned} d\phi_0/dt &= -\nabla\phi_0\cdot\mathbb{D}\cdot\nabla\phi_0 \\ &= -\mathbb{F}\cdot\mathbb{D}^{-1}\cdot\mathbb{F}+\mathbb{V}\cdot\mathbb{D}^{-1}\cdot\mathbb{V}. \end{aligned} \tag{20}$$

In evolution, the diffusion matrix $\mathbb{G}$ has special biological meaning describing the sampling nature of the genetic drift (for example, random mating for sexual species). So, we are naturally interested in the $\phi_0(\mathbb{G})$ and $d\phi_0(\mathbb{G})/dt$. We will see the $d\phi_0(\mathbb{G})/dt$ is related to the genetic variance and it generalizes the Fisher's FTNS.

We can see in the subspace for the ith species (details in Appendixes),

$$V_A(w^{(i)})/(\bar{w}^{(i)})^2=\ 2(\epsilon^{(i)})^{-1}\mathbb{F}^{(i)}\cdot(\mathbb{G}^{-1})^{(i)}\cdot\mathbb{F}^{(i)}, \tag{21}$$

where $V_A(w^{(i)})=2\sum_{k=1}^{n_i}\mathbb{X}_k^{(i)}(w_k^{(i)}-\bar{w}^{(i)})^2$. We take the sum with respect to i to obtain $\mathbb{F}\cdot\mathbb{G}^{-1}\cdot\mathbb{F}=(1/2)\sum_{i=1}^{N}\epsilon^{(i)}V_A(w^{(i)})/(\bar{w}^{(i)})^2$. Finally, we obtain

$$\frac{d\phi_0(\mathbb{G})}{dt}=-\frac{1}{2}\sum_{i=1}^{N}\epsilon^{(i)}\frac{V_A(w^{(i)})}{(\bar{w}^{(i)})^2}+\mathbb{V}(\mathbb{G})\cdot\mathbb{G}^{-1}\cdot\mathbb{V}(\mathbb{G}). \tag{22}$$

Specifically for the case of mono-species ($N=1$),

$$\frac{d\phi_0(\mathbf{G})}{dt}=-\frac{1}{2}\frac{V_A(w)}{\bar{w}^2}+\mathbf{V}(\mathbf{G})\cdot\mathbf{G}^{-1}\cdot\mathbf{V}(\mathbf{G}). \tag{23}$$

As mentioned before, the frequency-independent selection mono-species population system is in the equilibrium in which the intrinsic flux velocity $\mathbf{V}(\mathbf{G})=0$, and the intrinsic non-equilibrium potential $\phi_0=-(1/2)\ln\bar{w}$. Therefore, for the case of frequency-independent mono-species population system, Eq. (22) is simplified to the Fisher's FTNS, $d\bar{w}/dt=V_A(w)/\bar{w}$. We call Eq. (22) generalized FTNS which uncovers the underlying connection of adaptive rate with not only the genetic variance (as originally proposed by Fisher) related to the non-equilibrium intrinsic potential ϕ_0 but also the corresponding intrinsic flux velocity $\mathbb{V}$ (missing in Fisher's original FTNS). As we can see in the general evolution dynamics, the adaptation rate is not only determined by the genetic variance but also by the flux.

For evolution, Wright showed his mean fitness adaptive landscape gives the evolutionary optima and Fisher's fundamental theorem of natural selection gives the speed to approach the optima with adaptive rate of mean fitness which is related to the genetic variance. Fisher's FTNS implies that the mean fitness is a Lyapunov function (the mean fitness change rate is always non-negative) in the frequency-independent selection system. In this respect Fisher talked about the same thing as Wright except on different perspectives. Wright emphasizes on the local gradient dynamics

while Fisher emphasizes on the adaptive rate of the mean fitness being never negative. This all leads to the mean fitness being Lyapunov function. But, such picture breaks down in the general case, i.e., frequency-dependent selection system in which case there are interactions between individuals. We now know that in the general case there is such a Lyapunov function never increasing for the evolution and always searching for the optima. This is the emergent intrinsic landscape ϕ_0. But this Lyapunov function ϕ_0 in general is not the mean fitness originally proposed by Wright and Fisher. Only in the special case of frequency-independent selection, ϕ_0 reduces to the original Wright's fitness landscape. For the general case including the frequency-dependent selection, our newly defined non-equilibrium adaptive landscape is measured by the intrinsic potential function $\phi_0(\mathbb{G})$ and the adaptive rate by the $d\phi_0(\mathbb{G})/dt$ which is never positive ($\phi_0(\mathbb{G})$ never increasing). This is our picture about the natural selection and the adaptive landscape.

A. The Red Queen hypothesis explained by our generalized fundamental theorem of natural selection

What does our generalized FTNS imply? Insights can be gained by the case when $d\phi_0(\mathbb{G})/dt = 0$, in which the overall population system reaches its optima. For frequency-independent selection case, the population is in the detailed balance, i.e., $\mathbb{V}(\mathbb{G}) = 0$. Consequently, the genetic variance for every species $V_A(w^{(i)}) = 0$. The natural selection cannot change the allele frequency.

However, the intrinsic flux in general evolution dynamics is not equal to zero, i.e., for the evolution system with frequency-dependent selection. The non-zero intrinsic flux velocity, $\mathbb{V}(\mathbb{G}) \neq 0$, gives rise to $\sum_{i=1}^{N} \epsilon^{(i)} V_A(w^{(i)})/(\bar{w}^{(i)})^2 = 2\ \mathbb{V}(\mathbb{G}) \cdot \mathbb{G}^{-1} \cdot \mathbb{V}(\mathbb{G}) \geq 0$. The non-zero genetic variance implies additional natural selection have effects on some species to change the allele frequencies even if the overall population system reaches its optima. We explore further which species has the non-zero genetic variance. Since $\mathbb{G}$ is a block diagonal matrix, we can decompose the selection force acted on the ith species from Eq. (19) as the form: $\mathbb{F}^{(i)} = -\mathbb{G}^{(i)} \cdot (\nabla\phi_0)^{(i)} + \mathbb{V}^{(i)}$. Inserting it into Eq. (21) and using the orthogonality $\mathbb{V} \cdot \nabla\phi_0 = 0$, we get

$$V_A(w^{(i)}) = 2(\epsilon^{(i)})^{-1}(\bar{w}^{(i)})^2[(\nabla\phi_0)^{(i)} \cdot \mathbb{G}^{(i)} \cdot (\nabla\phi_0)^{(i)} + \mathbb{V}^{(i)} \cdot (\mathbb{G}^{-1})^{(i)} \cdot \mathbb{V}^{(i)}]. \quad (24)$$

When $d\phi_0(\mathbb{G})/dt = 0$, we have $\nabla\phi_0 = 0$. Therefore, we obtain

$$V_A(w^{(i)}) = 2(\epsilon^{(i)})^{-1}(\bar{w}^{(i)})^2[\mathbb{V}^{(i)} \cdot (\mathbb{G}^{-1})^{(i)} \cdot \mathbb{V}^{(i)}] \geq 0. \quad (25)$$

If the intrinsic flux flows into the ith subspace, the non-zero $\mathbb{V}^{(i)}$ gives rise to the genetic variance for ith species and sustains it. As a result, the ith species continually evolves even if the overall population is in its optima.

Then, what is the cause of the non-zero intrinsic flux velocity? For the overall population system, its evolution is affected by external physical environment and internal biotic interactions. If there is no biotic interaction, the natural selection from the external physical environment is frequency-independent selection which is a gradient force as given by Wright's picture. The non-zero intrinsic flux velocity results from the internal biotic interactions which can come from the same species or between different species. Of course, the external physical environment can also operate on the flux through coupling with the biotic interactions, but the biotic interaction is necessary. Therefore, we can see that the biotic interactions can sustain a genetic variation in fitness and thus give rise to endless evolution of some species. The effect caused by the interactions between different species was indicated by Van Valen as the Red Queen hypothesis.[4] According to this hypothesis, the biotic interactions between different species can lead to endless evolution processes for some species even if the physical environment is unchanged. The coevolving systems often enter into a limit cycle or chaos. Such phenomena is called Red Queen dynamics. Our potential and flux landscape theory provides a theoretical basis and quantitative explanation for this effect.

The maintenance of genetic variance by biotic interactions guarantees the rationality of the Red Queen hypothesis as the explanation of persistence of sexual reproduction. In a parasite-host system, their interactions can sustain a genetic variance which preserves the genotypic diversification in host population via sexual reproduction. The host species benefit from the genotypic diversification in resisting the parasites and thus the sexual reproduction can be persisted.[6,7]

The traditional evolutionary theory neglects the effects of biotic interactions on the evolutionary process. As the result, the evolutionary process is to adapt a fixed landscape (when the external physical environment is unchanged). Recently, the evolutionary game theory was proposed and developed to explore the coevolving systems.[39] According to the evolutionary game theory, the landscape of a biotic system is continually changed by coevolving other biotic systems.[40] In our potential-flux framework, we constructed Lyapunov function for the system to include all the biotic interactions. We can find the non-equilibrium intrinsic potential to construct the underlying adaptive landscape. The intrinsic potential landscape indicates where the evolutionary optima are. In addition, the intrinsic flux (need to be large enough, such as the limit cycle system) can drive some species into an endless cyclic evolution even though the optima has already been reached.

VI. DISCUSSION

Wright presented the mean fitness as adaptive landscapes, which he thought it to be a Lyapunov function so that evolution is always searching for optima. But this can be only applied to the simple case of frequency-independent selection system. Wright's evolutionary dynamics for the mean fitness is a gradient dynamics and therefore is in detailed balance. So Wright's adaptive fitness landscape corresponds to the evolution of an equilibrium system and mean fitness as a potential always tends to settles to the equilibrium optima. For the real and general evolutionary dynamics, the mean fitness does not always increase. So evolution does not always search for optima for mean fitness. Many people think that there is no general potential function existed always searching for optima for

evolution dynamics.[24] However, we show here that an intrinsic potential landscape ϕ_0 with Lyapunov function's property of always searching for optima does exist for evolution dynamics. The ϕ_0 is an emergence landscape from the evolution dynamics and not given *a priori*. With the Lyapunov nature, the ϕ_0 rather than the mean fitness never increases and always search for minima for the general evolution dynamics. So we found an optimal principle for evolution. In reality, since the external environment is constantly changing, the corresponding intrinsic landscape also changes accordingly. This results the changes or shifts of the optima.

Furthermore, the general evolution dynamics cannot be written simply as a pure gradient of a potential landscape as Wright's simple case. However, it can be determined by the gradient of a potential landscape and the additional curl probability flux as shown here. The curl probability flux is the missing part in the traditional evolutionary theory. In this work, we established a potential-flux landscape theory for evolutionary dynamics. While Wright's landscape is determined *a priori* by the mean fitness, our general evolution landscape is emergent from the whole dynamics of the system with both components of the potential and the flux which are not given *a priori*. We went beyond Wright's gradient dynamics and explore the general dynamics in non-equilibrium regime (for example, frequency-dependent selection) for evolution. The fitness flux was proposed recently, which is defined as the selective effect of the genotype frequency changes by using the fluctuation theorems in statistical physics.[23] Our curl flux is defined in a different way as the physical probability flux with divergent free curl nature and with the direct linkage to the non-equilibrium part of the evolutionary dynamics. There were studies for some specific cases of evolution from deterministic and stochastic dynamics perspectives,[12,16] the general evolutionary landscape from the underlying non-equilibrium nonlinear dynamical systems seems challenging to compute and obtain in practice with those approaches. In our theory, for a given evolution dynamics, we can straightforwardly quantitatively uncover the underlying potential landscape as well as the probability flux. The gradient and curl forces as a duality pair complement one another for the dynamics of evolution mimicking the an electron moving in an electric and magnetic field.

The limit cycle in evolution dynamics is often used as the argument against the existence of an underlying potential landscape searching for optima.[24] The claim is that, the limit cycle population repeatedly visits the same states in alternate generations shows that one cannot model all evolution in terms of some functions that increase every generation. As we see clearly here, on the contrary, such a function ϕ_0 with Lyapunov property of always decreasing does exist for the general evolution dynamics. On the limit cycle oscillation ring, the ϕ_0 is a constant while away from the oscillation path, the values of ϕ_0 are all higher, and the system is attracted to the oscillation ring due to the property of ϕ_0 always decreasing. The driving force for the coherent oscillation on the ring from one point to the other is not from gradient of the ϕ_0 since it is zero on the ring. Instead the curl probability flux drives the coherent oscillation on the ring. The dual contribution of the potential gradient and curl flux provides the foundation for coherent limit cycle oscillations in evolution dynamics. Potential gradient attracts the system down to the oscillation ring and curl flux drives the coherent oscillation on the ring.

We investigated the general evolution dynamics of a biological example of a group help model with frequency-dependent selection. We explored the underlying potential-flux landscape. We found the quantitative criterion for global stability from landscape topography. These explain how the evolutionary dynamics can be robust and stable under different conditions and environments.

We quantified the evolution pathways. The evolutional paths do not follow the normally expected steepest descent gradient path on the landscape and do not necessarily pass the saddle point or transition state. The evolution paths are irreversible due to the non-zero flux. This implies the flux has significant impact on the evolution path in addition to potential gradient and is the source of the irreversibility.

When the adaptive rate is measured by intrinsic potential landscape rather than mean fitness, we generalize the Fisher's FTNS linking adaptive rate and genetic variance, including the frequency-dependent selection, and decompose the contribution of the adaptive rate to not only the genetic variance related to the intrinsic potential but also the flux velocity. This shows the importance of the potential-flux landscape for the evolutionary dynamics.

As a result of the generalized FTNS, we discussed about the Red Queen phenomena. In our potential-flux landscape framework, we can clearly see the origin of the Red Queen phenomena. The endless evolution comes from the non-zero flux from the biotic interactions even when the evolution potential reaches the optima. So Van Valen's Red Queen hypothesis is the biological expression of the intrinsic flux: the system lies in the optimum where the gradient of potential is zero, but the intrinsic flux drives the endless evolution. As Van Valen himself remarked, this cannot be explained by traditional evolutionary theory, since the flux is the missing part of the traditional evolutionary theory.

In summary, our newly defined adaptive landscape is quantified by the intrinsic potential $\phi_0(\mathbb{G})$ and the adaptive rate by $d\phi_0(\mathbb{G})/dt$ which is never positive. The adaptation is realized through the minimization process of the intrinsic potential. This is our interpretation for evolutionary adaptation.

The non-equilibrium potential-flux landscape is important for exploring global natures of the general dynamical system. It is not only suitable for the biological evolutionary process, which is important for human health issues such as diseases like cancers from perspectives of evolution and networks, but also applicable to other biological and physical complex systems.

ACKNOWLEDGMENTS

F.Z., L.X., K.Z., and E.K.W. would like to thank financial supports from National Natural Science Foundation of China (NSFC) (Grant Nos. 21190040 and 11174105, 973 project 2009CB930100 and 2010CB933600). J.W. thanks National Science Foundation (NSF) for supports.

APPENDIX A: ABOUT THE RED QUEEN HYPOTHESIS

The traditional evolutionary theory is often described as "survival of the fittest." For instance, chilliness has removed the weak trees and left the strong. On the contrary, in the bee population, the weak bees can also survive against the chilliness. This can be due to the help from the kin group. Obviously, the interactions among individuals result in an important consequence: the population generally does not necessarily evolve towards the mean fitness maximum.

The Red Queen hypothesis emphasizes the effect of interactions among different species on their evolution. The parasite-host interaction system operates as predicted by Red Queen hypothesis. Parasites live and multiply inside their hosts and cause disease in the hosts, while hosts defend against the invasion of parasites. There is specificity between immunity of host and virulence of parasites. Now the most parasites have the V1 type virulence. The hosts who have the corresponding I1 type immunity can resist parasites and thus reproduce while other type hosts die and do not reproduce. After one generation, the parasites cannot infect the hosts so that they need to generate new virulence V2 for reproduction and thus the hosts evolve new immunity I2. The virulence of parasites and immunity of hosts continually improve. Consequently, the competition between the hosts and parasites are endless.

In Lewis Carroll's "*Through the Looking Glass*,"[41] Red Queen tells Alice: "it takes all the running you can do to keep in the same place." The endless coevolution is just like it. But the underlying mechanism is unclear and thus Van Valen refers to as "Red Queen hypothesis."[4]

APPENDIX B: DERIVATIVE OF FREE ENERGY WITH RESPECT TO TIME

The intrinsic free energy of the non-equilibrium system is defined as

$$\mathcal{F} = \mathcal{E} - \mathcal{D}S = \mathcal{D}\left(\int \mathcal{P}\ln(\mathcal{P}/\mathcal{P}_{ss})d\mathbf{x} - \ln\mathcal{Z}\right), \quad \text{(B1)}$$

where $\mathcal{Z} = \int \exp(-\phi_0/\mathcal{D})d\mathbf{x}$ is the intrinsic partition function which is not dependent on time t.

$$\begin{aligned}\frac{d\mathcal{F}}{dt} &= \mathcal{D}\frac{d}{dt}\left(\int \mathcal{P}\ln\left(\frac{P}{\mathcal{P}_{ss}}\right)d\mathbf{x}\right)\\ &= \mathcal{D}\int \frac{d\mathcal{P}}{dt}\ln\left(\frac{\mathcal{P}}{\mathcal{P}_{ss}}\right)d\mathbf{x} + \mathcal{D}\int \frac{d\mathcal{P}}{dt}d\mathbf{x}\\ &= -\mathcal{D}\int(\nabla\cdot\mathcal{J})\ln\left(\frac{\mathcal{P}}{\mathcal{P}_{ss}}\right)d\mathbf{x} + \mathcal{D}\frac{d}{dt}\int \mathcal{P}d\mathbf{x}\\ &= -\mathcal{D}\left(\int \nabla\cdot\left[\mathcal{J}\ln\left(\frac{\mathcal{P}}{\mathcal{P}_{ss}}\right)\right]d\mathbf{x} - \int \mathcal{J}\cdot\nabla\ln\left(\frac{\mathcal{P}}{\mathcal{P}_{ss}}\right)d\mathbf{x}\right).\end{aligned} \quad \text{(B2)}$$

Here, $\mathcal{J}$ is defined as $\mathcal{J} = \mathbf{J}|_{D\to 0}$. We use the Gauss's theorem and the boundary condition $\mathbf{n}\cdot\mathbf{J} = 0$ (which is result of conservation of total probability) to obtain

$$\frac{d\mathcal{F}}{dt} = \mathcal{D}\left(\int \mathcal{J}\cdot\nabla\ln\left(\frac{\mathcal{P}}{\mathcal{P}_{ss}}\right)d\mathbf{x}\right). \quad \text{(B3)}$$

From $\mathbf{J} = \mathbf{F}P - D\nabla\cdot(\mathbf{D}P) = (\mathbf{F} - D\nabla\cdot\mathbf{D} - D\mathbf{D}\cdot\nabla\ln P)P$, we can get

$$\mathcal{J}/\mathcal{P} + \mathcal{D}\mathbf{D}\cdot\nabla\ln\mathcal{P} = \mathcal{J}_{ss}/\mathcal{P}_{ss} + \mathcal{D}\mathbf{D}\cdot\nabla\ln\mathcal{P}_{ss}. \quad \text{(B4)}$$

Consequently, we get

$$\mathcal{J} = \mathcal{P}[\mathcal{J}_{ss}/\mathcal{P}_{ss} - \mathcal{D}\mathbf{D}\cdot\nabla\ln(\mathcal{P}/\mathcal{P}_{ss})]. \quad \text{(B5)}$$

So,

$$\begin{aligned}\frac{d\mathcal{F}}{dt} &= \mathcal{D}\left(\int \mathcal{P}\left[\frac{\mathcal{J}_{ss}}{\mathcal{P}_{ss}} - \mathcal{D}\mathbf{D}\cdot\nabla\ln\left(\frac{\mathcal{P}}{\mathcal{P}_{ss}}\right)\right]\cdot\nabla\ln\left(\frac{\mathcal{P}}{\mathcal{P}_{ss}}\right)d\mathbf{x}\right)\\ &= \mathcal{D}\left(\int \mathcal{P}\frac{\mathcal{J}_{ss}}{\mathcal{P}_{ss}}\cdot\nabla\ln\left(\frac{\mathcal{P}}{\mathcal{P}_{ss}}\right)d\mathbf{x}\right) - \mathcal{D}^2\left(\int\left[\nabla\ln\left(\frac{\mathcal{P}}{\mathcal{P}_{ss}}\right)\cdot\mathbf{D}\cdot\nabla\ln\left(\frac{\mathcal{P}}{\mathcal{P}_{ss}}\right)\right]\mathcal{P}d\mathbf{x}\right)\\ &= \mathcal{D}\left(\int \mathcal{J}_{ss}\cdot\nabla\left(\frac{\mathcal{P}}{\mathcal{P}_{ss}}\right)d\mathbf{x}\right) - \mathcal{D}^2\left(\int\left[\nabla\ln\left(\frac{\mathcal{P}}{\mathcal{P}_{ss}}\right)\cdot\mathbf{D}\cdot\nabla\ln\left(\frac{\mathcal{P}}{\mathcal{P}_{ss}}\right)\right]\mathcal{P}d\mathbf{x}\right)\\ &= \mathcal{D}\left(\int \nabla\cdot\left(\mathcal{J}_{ss}\frac{\mathcal{P}}{\mathcal{P}_{ss}}\right)d\mathbf{x} - \int \frac{\mathcal{P}}{\mathcal{P}_{ss}}\nabla\cdot\mathcal{J}_{ss}d\mathbf{x}\right) - \mathcal{D}^2\left(\int\left[\nabla\ln\left(\frac{\mathcal{P}}{\mathcal{P}_{ss}}\right)\cdot\mathbf{D}\cdot\nabla\ln\left(\frac{\mathcal{P}}{\mathcal{P}_{ss}}\right)\right]\mathcal{P}d\mathbf{x}\right)\\ &= \mathcal{D}\left(\int \nabla\cdot\left(\mathcal{J}_{ss}\frac{\mathcal{P}}{\mathcal{P}_{ss}}\right)d\mathbf{x} - \int \frac{\mathcal{P}}{\mathcal{P}_{ss}}\frac{\partial\mathcal{P}_{ss}}{\partial t}d\mathbf{x}\right) - \mathcal{D}^2\left(\int\left[\nabla\ln\left(\frac{\mathcal{P}}{\mathcal{P}_{ss}}\right)\cdot\mathbf{D}\cdot\nabla\ln\left(\frac{\mathcal{P}}{\mathcal{P}_{ss}}\right)\right]\mathcal{P}d\mathbf{x}\right)\\ &= \mathcal{D}\left(\int \nabla\cdot\left(\mathcal{J}_{ss}\frac{\mathcal{P}}{\mathcal{P}_{ss}}\right)d\mathbf{x}\right) - \mathcal{D}^2\left(\int\left[\nabla\ln\left(\frac{\mathcal{P}}{\mathcal{P}_{ss}}\right)\cdot\mathbf{D}\cdot\nabla\ln\left(\frac{\mathcal{P}}{\mathcal{P}_{ss}}\right)\right]\mathcal{P}d\mathbf{x}\right).\end{aligned} \quad \text{(B6)}$$

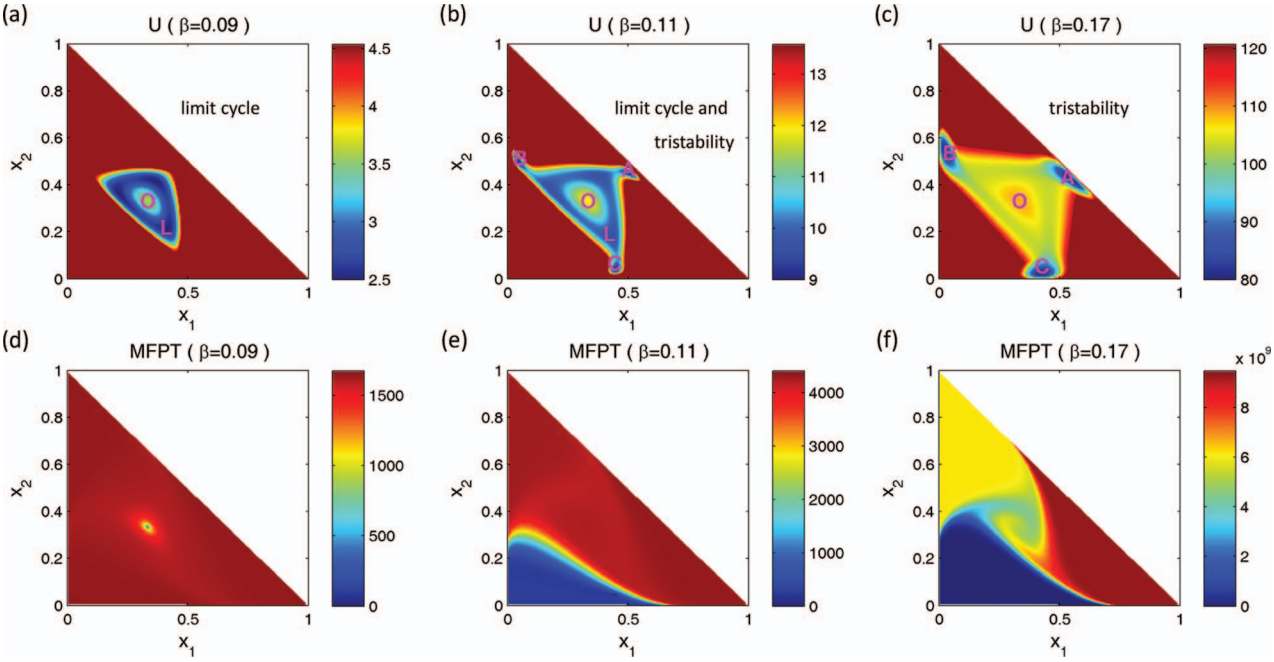

FIG. 6. Population potential landscape and corresponding MFPT with $D = 3 \times 10^{-4}$. (a) The population potential landscape for $\beta = 0.09$. (b) The population potential landscape for $\beta = 0.11$. (c) The population potential landscape for $\beta = 0.17$. (d) The MFPT from any state to the stable state O for the case of $\beta = 0.09$. (e) The MFPT from any state to the stable state C for the case of $\beta = 0.11$. (f) The MFPT from any state to the stable state C for the case of $\beta = 0.17$.

We also use the Gauss's theorem and the boundary condition $\mathbf{n} \cdot \mathbf{J} = 0$ (which is result of conservation of total probability) to obtain

$$\frac{d\mathcal{F}}{dt} = -\mathcal{D}^2 \int \nabla \ln\left(\frac{\mathcal{P}}{\mathcal{P}_{ss}}\right) \cdot \mathbf{D} \cdot \nabla \ln\left(\frac{\mathcal{P}}{\mathcal{P}_{ss}}\right) \mathcal{P} d\mathbf{x}. \quad \text{(B7)}$$

Due to the positive definite diffusion matrix $\mathbf{D}$,

$$\frac{d\mathcal{F}}{dt} \leq 0. \quad \text{(B8)}$$

APPENDIX C: MEAN FIRST PASSAGING TIME

We can use the equation of MFPT to describes the transition time τ from any state $\mathbf{x}$ to a given final state:[31]

$$\mathbf{F} \cdot \nabla \tau + D \nabla \tau \cdot \mathbf{D} \cdot \nabla \tau = -1. \quad \text{(C1)}$$

The boundary condition is taken as an absorbing boundary condition $\tau = 0$ at the final site and reflecting boundary conditions $\mathbf{n} \cdot \nabla \tau = 0$ for the outer boundary. We denote the transition time from A to B by τ_{AB}. We obtain the numerical solution of above equation.

Figure 6 shows the population potential landscape and corresponding MFPT with the fluctuation strength $D = 3 \times 10^{-4}$. Figures 6(a)– 6(c) show the potential landscape for $\beta = 0.09$, $\beta = 0.11$, and $\beta = 0.17$, respectively. In Figs. 6(a)–6(c), $O(1/3, 1/3)$ is the local maximum point (the top of the Mexican hat). In Figs. 6(a) and 6(b), L is the one of minimum on limit cycle. In Figs. 6(b) and 6(c), A, B, and C are the three stable states. Figure 6(d) shows the distribution of transition time from any state to the state O. Figures 6(e) and 6(f) show the distribution of transition time from any state to the a stable state C.

APPENDIX D: PHASE COHERENCE

We can discuss the coherence of the oscillation with respect to the diffusion coefficient D and other parameters. This can be quantified by the phase coherence ξ which quantitatively measures the degree of persistence for the progression of the oscillations. ξ is defined as follows: Choose the vector $N(t) = n_1(t)e_1 + n_2(t)e_2$ as shown in Fig. 7(a). The unit vectors chosen are $e_1 = (0, 1)$ and $e_2 = (1, 0)$. $n_1(t)$ and $n_2(t)$ are the frequency of the two alleles at time t. Then $\omega(t)$ is the phase angle between $N(t)$ and $N(t + \tau)$, where τ should be chosen to be smaller than the deterministic period and larger than the fast fluctuations. We choose $\tau = 0.1$. $\omega(t) > 0$ implies that the oscillation proceeds in the positive direction (counterclockwise). The formula of ξ is given as[42]

$$\xi = \frac{2\sum_i [\theta(\omega(t_i))\, \omega(t_i)]}{\sum_i |\omega(t_i)|} - 1, \quad \text{(D1)}$$

where $\theta(\omega) = 1$ if $\omega(t_i) > 0$, and $\theta(\omega) = 0$ if $\omega(t_i) \leq 0$. The sums are taken over every time step for the simulation trajectory. $\xi \approx 0$ implies that the system moves stochastically and has no coherence. The oscillation is mostly coherent when $|\xi|$ is close to 1. Fig. 7(b) shows that the coherence decreases when the fluctuation becomes stronger in GHM.

APPENDIX E: THE EVOLUTION PATHWAYS

The evolution pathways can be quantified and mathematically formulated by the general non-equilibrium path integral method we developed.[36] The general formulation and computing strategy of the non-equilibrium paths developed

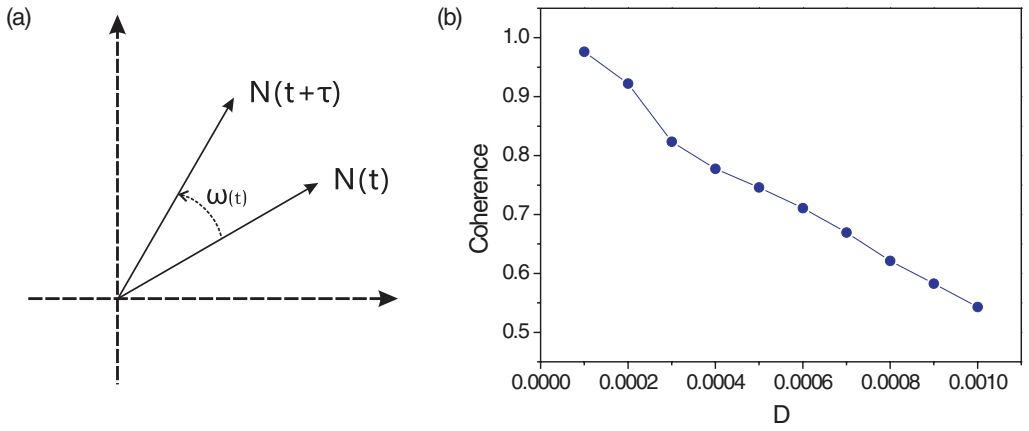

FIG. 7. (a) Sketch map for the definition of phase coherence ξ. (b) The coherence versus fluctuation strength D in GHM.

by us earlier can be directly applied to the evolution dynamics here. We follow this recipe and obtain the dominant evolution paths by optimizing the action or the Lagrangian of the system. There are technical challenges for the optimization. Therefore we transformed the path integral into the Hamilton-Jacobian representation. In this way, the computation challenge for the dominant evolution pathways is simplified to a key component which is the canonical momentum of the system integrated along a one dimensional line. This is numerically manageable. The readers who are interested in mathematical details can go through our paper for the optimization of the Lagrangian, Hamilton-Jacobian approach for the quantifications of the dominant evolution pathways.[36]

We calculate the evolutionary pathways for the GHM model. Figure 5 shows the case of zero fluctuation limit and Fig. 8 shows the dominant pathways with the finite fluctuation strength $D = 3 \times 10^{-4}$. We can also see clearly that evolution pathways do not follow the gradient paths on the underlying potential landscape. This results from the non-zero flux.

APPENDIX F: THE RELATIONSHIP BETWEEN ADDITIVE GENETIC VARIANCE AND NATURAL SELECTION

The natural selection force is given by

$$F_i^S = \frac{x_i(w_i - \bar{w})}{\bar{w}}, \tag{F1}$$

with $\sum_{i=1}^{n} F_i^S = 0$. The inverse matrix of $\mathbf{G} = \{x_i(\delta_{ij} - x_j) \mid 1 \le i, j \le (n-1)\}$ is known to have the property,

$$(\mathbf{G}^{-1} \cdot \mathbf{F})_i = \frac{F_i}{x_i} - \frac{F_n}{x_n}, \tag{F2}$$

where $F_n = -\sum_{i=1}^{n-1} F_i$. So, we have

$$\frac{V_A(w)}{\bar{w}^2} = \frac{2}{\bar{w}} \sum_i^n \frac{x_i(w_i - \bar{w})}{\bar{w}}(w_i - \bar{w})$$

$$= \frac{2}{\bar{w}} \sum_i^n F_i^S(w_i - \bar{w})$$

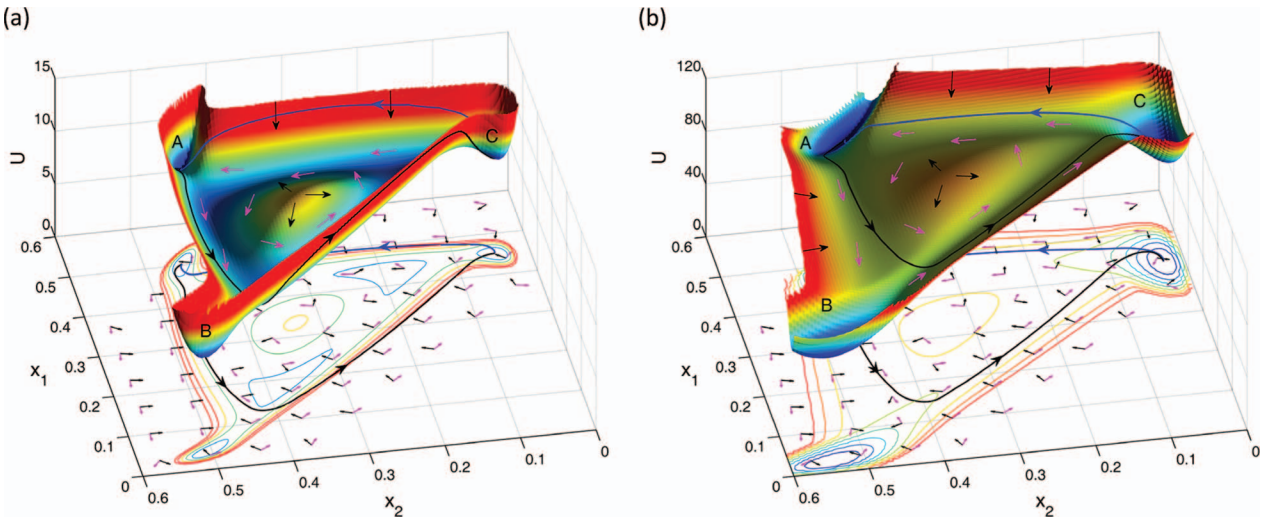

FIG. 8. The evolutionary pathways on the population potential landscape U with $D = 3 \times 10^{-4}$. ((a): $\beta = 0.11$ for limit cycle and tristability coexisting phase. (b): $\beta = 0.17$ for tristability phase.)

$$
\begin{aligned}
&= \frac{2}{\bar{w}}\left[\sum_i^n F_i^S w_i - \bar{w}\sum_i^n F_i^S\right] \\
&= \frac{2}{\bar{w}}\left[\left(\sum_i^{n-1} F_i^S w_i\right) + F_n^S w_n\right] \\
&= \frac{2}{\bar{w}}\left[\left(\sum_i^{n-1} F_i^S w_i\right) - \left(\sum_i^{n-1} F_i^S\right) w_n\right] \\
&= \frac{2}{\bar{w}}\sum_i^{n-1} F_i^S (w_i - w_n) \\
&= \frac{2}{\bar{w}}\sum_i^{n-1} F_i^S \bar{w}\left(\frac{F_i^S}{x_i} - \frac{F_n^S}{x_n}\right) \\
&= 2\mathbf{F}^S \cdot \mathbf{G}^{-1} \cdot \mathbf{F}^S. \qquad \text{(F3)}
\end{aligned}
$$

[1] C. Darwin, *On the Origin of Species by Means of Natural Selection* (Murray, London, 1859).
[2] R. A. Fisher, *The Genetical Theory of Natural Selection* (Oxford University Press, Oxford, 1930).
[3] S. Wright, "The roles of mutation, inbreeding crossbreeding and selection in evolution," in *Proceedings of the Sixth International Congress on Genetics* (Brooklyn Botanic Garden, Brooklyn, NY, 1932), Vol. 1, p. 356.
[4] L. Van Valen, Evol. Theory **1**, 1 (1973).
[5] G. Bell, *The Masterpiece of Nature: The Evolution and Genetics of Sexuality* (Croom Helm, London, 1982).
[6] W. D. Hamilton, R. Axelrod, and R. Tanese, Proc. Natl. Acad. Sci. U.S.A. **87**, 3566 (1990).
[7] M. Salathe, R. D. Kouyos, and S. Bonhoeffer, Trends Ecol. Evol. **23**, 439 (2008).
[8] C. M. Lively, C. Craddock, and R. C. Vrijenhoek, Nature (London) **344**, 864 (1990).
[9] S. Paterson, T. Vogwill, A. Buckling, R. Benmayor, and A. J. e. a. Spiers, Nature (London) **464**, 275 (2010).
[10] L. T. Morran, O. G. Schmidt, I. A. Gelarden, R. C. Parrish, and C. M. Lively, Science **333**, 216 (2011).
[11] M. Ridley, *Evolution* (Blackwell, 2004).
[12] S. A. Kauffman, *The Origins of Order: Self Organization and Selection in Evolution* (Oxford University Press, 1993).
[13] H. Haken, *Advanced Synergetics: Instability Hierarchies of Self-Organizing Systems and Devices* (Springer, Berlin, 1987).
[14] R. Graham, "Macroscopic potentials, bifurcations and noise in dissipative systems," in *Noise in Nonlinear Dynamical Systems*, edited by F. Moss, and P. McClintock (Cambridge University Press, 1989), Vol. 1, p. 225.
[15] M. Sasai and P. G. Wolynes, Proc. Natl. Acad. Sci. U.S.A. **100**, 2374 (2003).
[16] P. Ao, Commun. Theor. Phys. **49**, 1073 (2008).
[17] H. Qian, Methods Enzymol. **467**, 111 (2009).
[18] J. Wang, B. Huang, X. F. Xia, and Z. R. Sun, PLOS Comput. Biol. **2**, e147 (2006).
[19] K. Y. Kim and J. Wang, PLOS Comput. Biol. **3**, e60 (2007).
[20] S. Lapidus, B. Han, and J. Wang, Proc. Natl. Acad. Sci. U.S.A. **105**, 6039 (2008).
[21] J. Wang, L. Xu, and E. K. Wang, Proc. Natl. Acad. Sci. U.S.A. **105**, 12271 (2008).
[22] J. Wang, C. H. Li, and E. K. Wang, Proc. Natl. Acad. Sci. U.S.A. **107**, 8195 (2010).
[23] V. Mustonen and M. Lassig, Proc. Natl. Acad. Sci. U.S.A. **107**, 4248 (2010).
[24] S. H. Rice, *Evolutionary Theory: Mathematical and Conceptual Foundations* (Sinauer Associates, 2004).
[25] Y. M. Svirezhev and V. P. Passekov, *Fundamentals of Mathematical Evolutionary Genetics* (Kluwer Academic, Dordrecht, 1990).
[26] J. F. Crow and M. Kimura, *An Introduction to Population Genetics Theory* (Harper & Row, New York, 1970).
[27] J. Schnakenberg, Rev. Mod. Phys. **48**, 571 (1976).
[28] G. Nicolis and I. Prigogine, *Self-Organization in Nonequilibrium Systems* (Wiley, New York, 1977).
[29] C. Van den Broeck and M. Esposito, Phys. Rev. E **82**, 011144 (2010).
[30] H. Ge and H. Qian, Phys. Rev. E **81**, 051133 (2010).
[31] N. G. Van Kampen, *Stochastic Processes in Physics and Chemistry* (Elsevier, Amsterdam, 2007).
[32] G. Hu, Z. Phys. B: Condens. Matter **65**, 103 (1986).
[33] M. Eigen and P. Schuster, *The Hypercycle* (Springer, Berlin, Heidelberg, 1979).
[34] J. Hofbauer and K. Sigmund, *Evolutionary Games and Population Dynamics* (Cambridge University Press, 1998).
[35] I. M. Mitchell, J. Sci. Comput. **35**, 300 (2008).
[36] J. Wang, K. Zhang, and E. Wang, J. Chem. Phys. **133**, 125103 (2010).
[37] J. Wang, K. Zhang, L. Xu, and E. K. Wang, Proc. Natl. Acad. Sci. U.S.A. **108**, 8257 (2011).
[38] G. R. Price, Ann. Hum. Genet. **36**, 129 (1972).
[39] J. Maynard Smith and G. R. Price, Nature (London) **246**, 15 (1973).
[40] M. A. Nowak and K. Sigmund, Science **303**, 793 (2004).
[41] L. Carroll, *Through the Looking Glass* (Macmillan, London, 1871).
[42] M. Yoda, T. Ushikubo, W. Inoue, and M. Sasai, J. Chem. Phys. **126**, 115101 (2007).